
Paper 1

Petra Drevenšek, Janez Košmrlj, Gerald Giester, **Tormod Skauge**, Einar Sletten, Kristina Sepčić and Iztok Turel.

"X-Ray Crystallographic, NMR and Antimicrobial Activity Studies of Magnesium Complexes of Fluoroquinolones - Racemic Ofloxacin and Its *S*-form, Levofloxacin"

Journal of Inorganic Biochemistry (in print)

X-Ray Crystallographic, NMR and Antimicrobial Activity Studies of Magnesium Complexes of Fluoroquinolones - Racemic Ofloxacin and Its *S*-form, Levofloxacin.

Petra Drevenšek,[a] Janez Košmrlj,[a] Gerald Giester,[b] Tormod Skauge,[c] Einar Sletten,[c] Kristina Sepčić[d] and Iztok Turel*[a]

[a] Faculty of Chemistry and Chemical Technology, University of Ljubljana, Aškerčeva 5, SI-1000 Ljubljana, Slovenia.
[b] Institut für Mineralogie und Kristallographie, Geozentrum, Universität Wien, Althanstrasse 14, A-1090 Wien, Austria.
[c] Department of Chemistry, University of Bergen, Allégaten 41, 5007 Bergen, Norway.
[d] Biotechnical Faculty, Department of Biology, University of Ljubljana, Večna pot 111, 1000 Ljubljana, Slovenia.

*To whom correspondence should be addressed: Fax: 00 3861 2419220; Tel: 00 3861 2419124; E-mail: iztok.turel@fkkt.uni-lj.si

The magnesium complexes of racemic ofloxacin (oflo) and its pure *S*-form levofloxacin (*S*-oflo) have been studied by X-ray crystallography and NMR spectroscopy. Two compounds, $[Mg(R\text{-oflo})(S\text{-oflo})(H_2O)_2]\cdot 2H_2O$ (**1**) and $[Mg(S\text{-oflo})_2(H_2O)_2]\cdot 2H_2O$ (**2**), respectively, have been prepared by hydrothermal reactions and their crystal structures have been determined. The crystals are isomorphous (monoclinic $P2_1$). In both structures the anionic fluoroquinolone ligands are coordinated through the keto and carboxylate oxygens forming 1:2 Mg:oflo complexes. The two structures are practically identical except for the orientation of one of the oxazine methyl groups at the chiral center of **2** which was found in equatorial position, the other oxazine methyl groups in **1** and **2** being axial. This difference affects the stacking pattern of quinolone molecules in the cell. ^{1}H NMR chemical shift data and Mn(II) paramagnetic line broadening measurements on the free ofloxacin suggest that the coordination of the ligands in solution involves the keto and carboxylate oxygens. However, it is not possible to decide whether the complexes in aqueous solution have 1:1 or 1:2 stoichiometry. The methylated piperazine nitrogen does not interact with the metal ion. Magnesium-quinolone interaction is discussed in relation to the biological activity of quinolones. The antimicrobial activity of the complexes against various microorganisms was tested and it was established that their activity is similar to that of free quinolone drugs.

Key words: antibiotics / magnesium / X-ray diffraction / NMR spectroscopy / biological activity

Introduction

The research and development of quinolone antibacterial agents have seen an enormous worldwide effort for more than forty years. Over 10000 structurally related compounds have been isolated and described in patents and scientific papers [1]. Several fluoroquinolones in clinical use feature a carboxyl group at position 3, a keto group at position 4, a fluorine at position 6, and a piperazinyl or methyl piperazinyl group at position C-7. Differences at the moiety present at the N-1 and at the C-7 position markedly influence the microbiological activity and pharmacokinetic properties [2]. The ofloxacin molecule possesses an oxazine ring in which positions C-8 and N-1 are linked via the ring structure (Scheme 1). Attached to this ring is a methyl group that can exist in two optically active forms, the *S*-isomer being up to two orders of magnitude more potent than the *R*-isomer. The phenomenon is surprising, since the difference in structure between the enantiomers is only the steric configuration of a presumably non-functional methyl group relative to the ring plane. Initially, only racemic ofloxacin was available as a drug, but has now largely been replaced by the optical *S*-isomer (*S*-oflo) (trade name levofloxacin) which is currently a leader on the quinolone drug market.

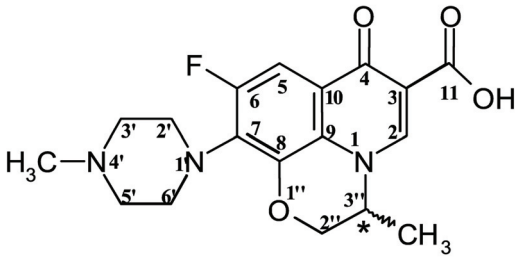

Scheme 1. Formulae of ofloxacin (*R*-, *S*-) or levofloxacin (*S*-) with numbering scheme (* denotes the chiral centre).

There are several families of antibiotics that require metal ions to function properly and were also dubbed ‘‘metalloantibiotics’’ [3]. Metal ions play a key role in the actions of metalloantibiotics and are involved in specific interactions of these antibiotics with various biomolecules (proteins, membranes, nucleic acids and other)**.** Magnesium (as a very common ion in biological systems) is not only important for the activity of quinolones but also for some other antibacterial agents, such as aureolic acid and derivatives, various tetracyclines and some other.

The target of the quinolones is the DNA gyrase, which changes negative superhelical coils into covalent circular DNA [4]. Both enantiomers have been found to bind to calf thymus DNA with higher affinity for the *S*-isomer than the *R*-isomer [5,6]. It is well-known that metal ions coordinate to quinolones, and several complexes have been isolated and characterized [7,8,9]. Antacids containing magnesium or aluminium markedly impair the absorption of orally administered fluroquinolones. The decrease in absorption may be as great as ten-fold. The mechanisms of action of various quinolones are not fully understood, but many of the theories focus on the involvement of magnesium ions [10,11,12,13,14,15]. It is not yet known whether the magnesium ion influence is due to its stabilizing effect on DNA topology or its ability to chelate with the keto and carboxylate moieties of quinolones.

Previously we have studied the interactions of magnesium and fluoroquinolones as well as the influence of magnesium on the interaction between fluoroquinolones and DNA oligodeoxyribonucleotides [16,17,18]. Here we report the crystal structures of [Mg(*R*-oflo)(*S*-oflo)$(H_2O)_2]\cdot 2H_2O$ (**1**) and [Mg(*S*-oflo)$_2(H_2O)_2]\cdot 2H_2O$ (**2**), ^{1}H NMR spectroscopic solution studies, and

antibacterial activity of the corresponding systems.

Experimental

Synthesis

[Mg(*R*-oflo)(*S*-oflo)(H_2O)$_2$]·2H_2O (1) and [Mg(*S*-oflo)$_2$(H_2O)$_2$]·2H_2O (2)

Compound **1** was synthesized by a hydrothermal reaction from a mixture of ofloxacin (0.126 g, 0.350 mmol), magnesium(II) chloride hexahydrate (35.6 mg) and L-histidine (27.2 mg) in the molar ratio of 2:1:1. Distilled water (1.0 mL) was added to the mixture of reactants and placed in a tube and pH was adjusted to 7 with 2M NaOH. The tube was then frozen by liquid nitrogen, evacuated and sealed. The ampoule was heated at 120 °C for 3 days to give pale yellow crystals of **1**. Yield: 8.9%. $C_{36}H_{46}F_2MgN_6O_{12}$: calcd. C 52.92, H 5.67, N 10.29; found: C 52.91, H 5.58, N 10.25. FTIR (cm^{-1}, Nujol): 3367(m), 1683(w), 1616(s), 1580(s), 1292(m), 1274(m), 1230(w), 1201(w), 1154(w), 1133(w), 1116(w), 1094(w), 1050(m), 1008(m), 982(m), 959(w), 940(w), 890(w), 843(w), 818(m), 786(w), 768(w), 747(w), 725(w), 694(w), 654(w), 632(w).

The procedure to prepare **2** was similar with the important difference that this synthesis was successful only in the absence of histidine. The amount of *S*-ofloxacin was 0.500 mmol (0.181 g), and 0.250 mmol (50.8 mg) of magnesium(II) chloride hexahydrate was added. The ampoule was heated at 130 °C for 1 day to give yellow crystals of **2**. Yield: 8.1%. $C_{36}H_{46}F_2MgN_6O_{12}$: calcd. C 52.92, H 5.67, N 10.29; found: C 52.91, H 5.69, N 10.29. FTIR (cm^{-1}, Nujol): 3354(m), 1692(w), 1614(s), 1576(s), 1290(m), 1273(m), 1230(w), 1199(w), 1152(w), 1133(w), 1114(w), 1081(m), 1069(m), 1046(m) 1008(m), 981(m), 959(w), 945(w), 895(w), 842(w), 818(m), 785(w), 766(w), 746(w), 725(w), 686(w), 655(w), 630(w).

Infrared spectra (Nujol) were recorded on a Perkin-Elmer FT-1720X spectrometer. The UV-VIS spectra were recorded on a Perkin-Elmer Lambda 6 UV/VIS spectrophotometer using 500 μL Quartz cuvettes (Hexxa) and pH was measured using a Sentron Argus pH meter equipped with a Sentron ISFET Hotline probe. Elemental analyzes were performed on a Perkin-Elmer 204C microanalyzer. The following chemicals were used: $MgCl_2·6H_2O$ (Fluka), levofloxacin (Fluka), ofloxacin (Sigma), L-histidine (Kemika, Zagreb). All were of analytical grade and used as supplied.

Crystallography

Crystal data and refinement parameters of compounds **1** and **2** are listed in Table 1. Intensity data were collected at 200 K for **1** and 150 K for **2**, respectively on Nonius Kappa CCD diffractometers equipped with a cooling device (Oxford Cryosystems, Cryostream Cooler), a Mo anode (λ = 0.71073 Å) and a graphite monochromator, and the multiscan absorption correction [19] was performed. The structures were solved by direct methods (SHELXS-97) and refined by a full-matrix least-squares procedure based on F^2 (SHELXL-97) [20]. Hydrogen atoms attached to water oxygen atoms were found in difference Fourier maps and were refined freely. All the remaining H atoms were placed at calculated positions and treated using appropriate riding models.

Structure **1** was initially solved in space group $P2_1/a$, as the intensity distribution favored a centrosymmetric cell. It was not, however, possible to refine the structure without invoking disorder in the piperazine ring region. A closer inspection of structure factors showed, that although *h0l* reflections with h = 2n+1 are generally weak, a sizeable fraction of these reflections violated the systematic extinction rule of $P2_1/a$. After conversion to the non-

centrosymmetric space group $P2_1$, the refinement of the structure proceeded nicely. The deviations from centrosymmetry are further discussed in the section on crystal structures. Determination of the absolute configuration through X-ray refinement was attempted for both structures. For compound **2**, where it is known chemically that both chiral centers are in the *S*-form, the refinement clearly favored the correct absolute configuration, even though the standard deviation in the Flack parameter is somewhat high, as is often found for light atom structures. Also in the case of **1**, which contains one *R*- and one *S*-ofloxacin group, the X-ray refinement resulted in a distinction between the two possible absolute structures.

CCDC-276067 (compound **1**) and CCDC-276068 (compound **2**) contain the supplementary crystallographic data for this paper. These data can be obtained free of charge at www.ccdc.cam.ac.uk/conts/retrieving.html [or from the Cambridge Crystallographic Data Centre, 12, Union Road, Cambridge CB2 1EZ, UK; fax: (internat.) +44-1223/336-033; E-mail: deposit@ccdc.cam.ac.uk].

Table 1. Crystal data and refinement parameters of compounds **1** and **2**.

	1	**2**
Formula	$C_{36}H_{46}F_2MgN_6O_{12}$	$C_{36}H_{46}F_2MgN_6O_{12}$
F_w	817.1	817.1
Crystal system	Monoclinic	Monoclinic
Space group	$P2_1$	$P2_1$
a (Å)	11.0244(3)	10.9761(4)
b (Å)	9.6181(2)	9.7345(4)
c (Å)	18.2476(9)	17.9179(8)
β(°)	97.999(3)	98.219(2)
V (Å^3), Z	1916.0(1), 2	1894.8(1), 2
T (K)	200(2)	150(2)
D_{calcd} (g cm^{-3})	1.416	1.432
μ(MoKα) (mm^{-1})	0.127	0.129
Crystal size (mm)	0.20 × 0.17 × 0.10	0.15 × 0.10 × 0.05
Crystal colour, shape	Yellow prism	Yellow prism
θ range (°)	3.45 – 26.37	3.45 – 26.37
Data measured, unique (R_{int})	15160, 7804 (0.0207)	14536,7654 (0.069)
Observed data [I>2σ(I)]	6624	5372
No. of parameters	547	547
R^a, $wR_2{}^b$ [I>2σ(I)]	0.0459, 0.1136	0.0489, 0.0914
R, wR_2 (all data)	0.0565, 0.1206	0.0927, 0.1078
S^c, $(\Delta/\sigma)_{max}$	1.019, 0.019	1.011, 0.001
Max, min peaks (eÅ^{-3})	0.926, -0.388	0.266, -0.237

[a] $R = \sum||F_o| - |F_c||/\sum|F_o|$. [b] $wR_2 = \{\sum[w(F_o^2 - F_c^2)^2]/\sum[w(F_o^2)^2]\}^{1/2}$. [c] $S = \{\sum[(F_o^2 - F_c^2)^2]/(n/p)\}^{1/2}$, where n is the number of reflections and p is the total number of parameters refined.

NMR Spectroscopy

Proton and carbon NMR spectra were recorded on Bruker DRX Avance 500, Avance 400 and Bruker Avance DPX 300 spectrometers operating at 500 MHz, 400 MHz and 300 MHz for ^{1}H NMR spectroscopy. 1D ^{1}H spectra were recorded typically using 160 transients collected with 32K data points at 298 K. Additional spectra were recorded at both higher and lower temperatures using 64-512 transients. 2D ^{1}H-^{13}C HSQC spectra were recorded at 298 K and 276 K. Typically 2048 complex points were collected in t_1 with 64-512 increments in t_2, where each increment was averaged over 256 transients. All spectra were referenced to the residual HDO resonance at 4.758 ppm at 298 K. NMR samples of the magnesium-quinolone complexes were prepared by dissolving 0.8 mg and 0.6 mg of **1** and **2**, respectively, in 0.8 mL 99.96 % D_2O (Cambridge Isotopes). The solutions were shaken at room temperature for 3 hours and centrifugated. Concentrations of the saturated solutions of complexes **1** and **2** were determined by UV spectroscopy. As the molar extinction coefficients for these complexes are unknown, the molar extinction coefficient for *S*-oflo, $\varepsilon = 23408\ cm^{-1}\ M^{-1}$, was used as reference [21]. This gave an approximate concentration of 0.14 mM and 0.31 mM for **1** and **2**, respectively. The UV spectra were practically identical, confirming the similarity of the two complexes in solution (data not shown). Of each centrifugate 500 μL were transferred to NMR tubes (Wilmad), pH 8.8. As reference solution, 1 mM free *S*-ofloxacin was used (in D_2O, pH 8.8). Mn(II) titration was carried out on a 1 mM *S*-ofloxacin solution using 0.5-20.0 mM $MnCl_2$ (Fluka) in aliquots of 2.5-10.0 μL.

Antimicrobial activity tests

The antibacterial potential of the magnesium complexes of levofloxacin and ofloxacin was assayed using three Gram positive (*Staphylococcus epidermidis*, *Micrococcus luteus*, *Bacillus subtilis*) and five Gram negative (*Salmonella enteritidis*, *Escherichia coli*, *Klebsiella pneumoniae*, *Pseudomonas aeruginosa*, *Enterococcus foecalis*) bacterial strains. All used bacteria were obtained from the local collection at the Department of Biology, University of Ljubljana.

Antimicrobial activities were evaluated using the agar diffusion test, as described earlier [22,23,24]. For estimation of minimal inhibitory concentration values (MIC), the antibacterial substances were gradually diluted in 50 mM Tris.HCl buffer pH 7.4. Free levofloxacin and ofloxacin, dissolved in the same buffer, were used as reference compounds.

Results and Discussion

Syntheses and Crystal Structures

It was previously reported that the presence of histidine in the preparation of quinolone metal complexes could result in the isolation of new crystalline products which are different from those obtained without using this compound [25]. In the present case histidine had to be added in order to obtain crystals of **1** while **2** crystallized in the absence of histidine. Histidine may serve to fine-tune the protolytic equilibria to reach the correct species distribution for crystallization. At pH 7 both *S*-oflo and *R*-oflo are present predominantly in neutral and zwitterionic forms (pKa_1= 6.0, pKa_2= 8.2) [26]. It was established (see above) by UV measurements in solution that the solubility of **2** is slightly higher than that of **1**.

The molecular structure of **2** is shown in Figure 1. Selected bond distances and angles are collected in Table 2. All bond distances and angles in both compounds are in agreement with corresponding data cited in the literature [7,27,28].

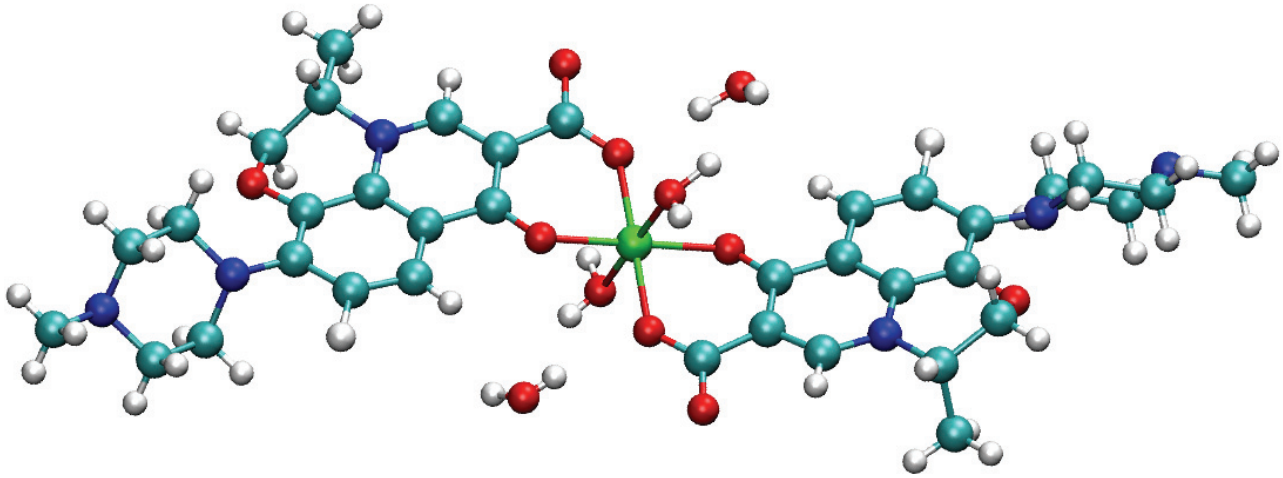

Figure 1. The molecular structure of **2**. The structure of **1** is practically superimposable except for the orientation of the oxazine methyl group (see below).

The common features of **1** and **2** are coordination to magnesium through the keto and carboxylate oxygens (Figure 1, Table 2). Quinolone molecules are in the anionic form. The slightly distorted octahedral coordination of magnesium is completed by two aqua ligands located in axial positions. The Mg – H_2O distances are significantly longer than the equatorial Mg – carboxyl/keto distances. The piperazine nitrogen does not interact with magnesium, probably due to the steric crowding of the methyl group. It is interesting to note that the hydrothermal reaction of quinolone norfloxacin (with non-methylated piperazine) with various metals at pH 7-8 resulted in a 2D square grid of complexes where also N-piperazine is coordinated to the metal [29,30].

Table 2. Selected geometric parameters of complexes **1** and **2** (Å,°).

	1	**2**
Mg—keto(a)	2.041(2)	2.033(2)
Mg—keto(b)	2.039(2)	2.029(2)
Mg— carboxyl (a)	2.032(2)	2.027(2)
Mg— carboxyl (b)	2.038(2)	2.038(3)
Mg— water (a)	2.086(2)	2.092(2)
Mg— water (b)	2.069(2)	2.077(2)
O(c,a)—Mg—O(k,a)	88.08(9)	87.87(10)
O(c,b)—Mg—O(k,a)	92.65(9)	93.42(9)
O(c,a)—Mg—O(k,b)	91.49(9)	91.09(9)
O(c,b)—Mg—O(k,b)	87.79(9)	87.56(9)
O(c,b)—Mg—O(w,i)	89.73(10)	88.88(11)
O(k,a)—Mg—O(w,i)	90.26(10)	88.03(10)
O(c,a)—Mg—O(w,ii)	89.97(10)	91.38(10)
O(k,a)—Mg—O(w,ii)	89.37(10)	90.95(10)
O(w,i)—Mg —O(w,ii)	179.52(14)	178.94(13)

k = keto; c = carboxyl; w = water

The aromatic ring systems of quinolone ligands are predominantly planar and piperazine rings are in the normal chair

conformation. The oxazine rings of *R*-oflo and *S*-oflo in **1** are almost planar. The main difference between structures **1** and **2** is related to the orientation of the oxazine methyl groups: one of the two oxazine methyl groups in **2** has adopted an equatorial orientation while all the other oxazine methyl groups are located in axial positions. The values of dihedral angles defining the orientation of the axial oxazine methyl group are in the range 76 -78^{o} which is significantly less than the average value of 87^{o} calculated for various metal free oxazine derivatives. The dihedral angle for the only methyl group found with equatorial orientation was determined at 20.1^{o}, significantly less than the calculated value of ~ 32° [31].

The crystal packing arrangements are as expected quite similar for **1** and **2** (Figure 2). The end-on view of the complexes (Fig. 2a) reveals that the quinolone planes are displaced to opposite sides of the equatorial coordination plane, and in addition there is a distinct propeller twist relative to this plane. Layers of overlapping quinolone rings are stabilized by weak π-π interactions (Fig. 2b). One feature that should be mentioned is that in **1** the perpendicular distance between layers is 4.32(7) Å, whereas in **2** this distance is significantly shorter (4.13(4) Å). This difference, which is due to the respective position of the oxazine methyl group in the two structures, may be important with regards to the ability of **1** and **2** to form stacked aggregates in solution.

Compound **1,** containing (*R*-oflo)(*S*-oflo) groups, was expected to crystallize in a centrosymmetric space group. However, in the course of the refinement (see crystallographic section) it became clear that the orientations of the two piperazine rings break this symmetry. The dihedral angle between best least-squares planes defined by the four carbon atoms of each ring is 89.1° (as opposed to 0° if Mg was positioned at a center of symmetry). This is practically identical to the corresponding dihedral angle found in **2** (89.9°). As described above, the crystal packing in both compounds is quite similar, with overlap between the two different parts of screw axis related molecules (Figure 2). The relative rotations of the piperazine rings seem to favour a denser packing; the deviation from centrosymmetry may hence be caused by packing effects.

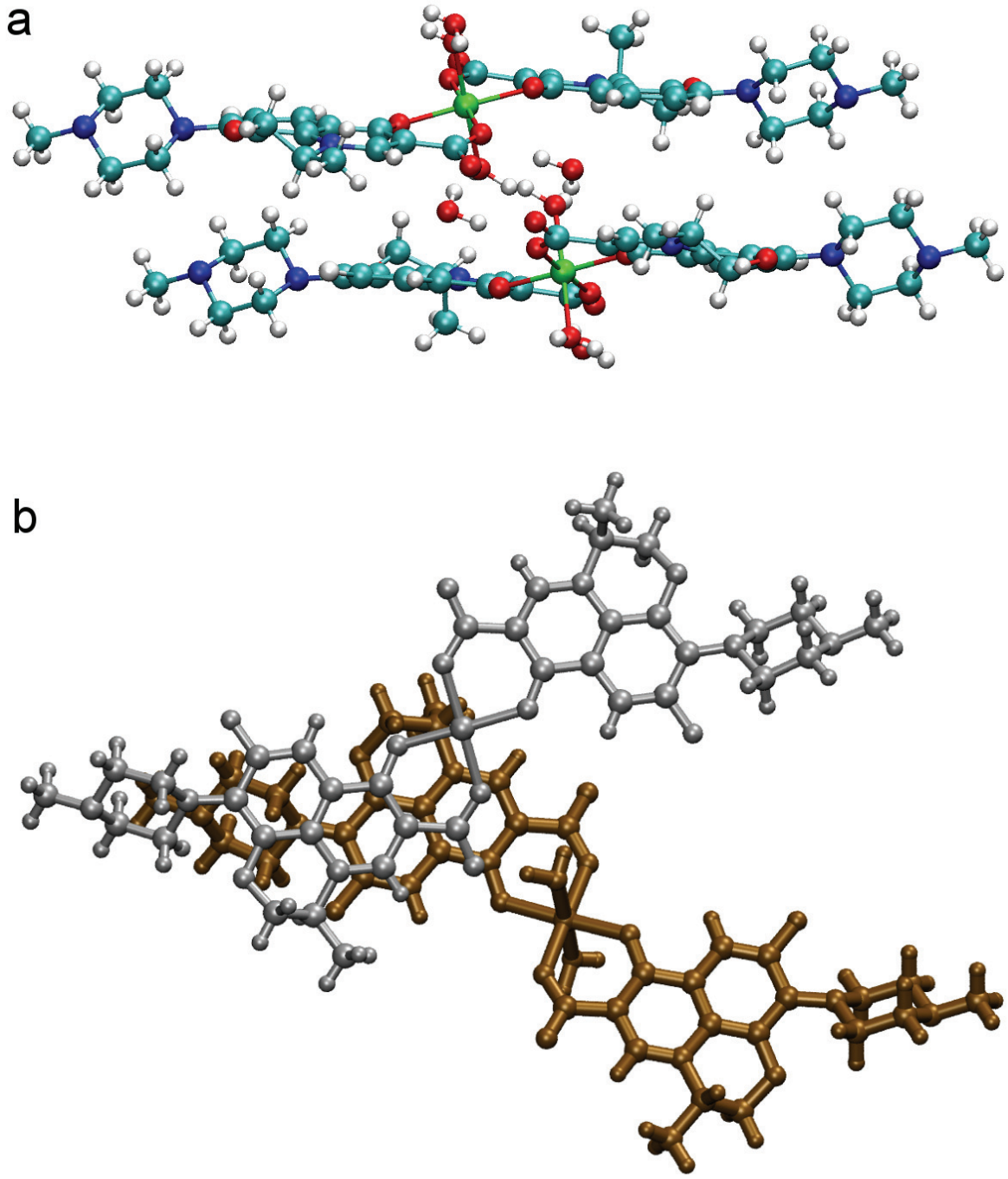

Figure 2. Crystal packing for **2**. Two complexes are present in each cell. Views parallel and perpendicular to the molecular plane.

NMR solution studies

The magnesium-quinolone complexes were studied by ^{1}H NMR and compared with the spectra of free quinolones. The solubility of the complexes around physiological pH was too low to obtain proton NMR spectra with sufficient signal-to-noise ratio. The spectra of free quinolones and the complexes **1** and **2** (Figure 3) exhibit the characteristic features of fluoroquinolone with two aromatic resonances around 7 – 8.5 ppm, the oxazine resonances close to the water resonance at 4 – 5 ppm, the piperazine resonances at 2.5 – 4 ppm, and at approximately 1.5 ppm the oxazine methyl resonance. The proton assignment was checked by 2D ^{1}H-^{13}C HSQC and HMBC experiments (data not shown) and is in agreement with previous work [17,32,33]. However, it was not possible to distinguish between H2´´a and H2´´b (Scheme 1) resonances and so far no reports have been given with an unambiguous assignment of these signals.

Shimada et al. [34] reported $\log K_1$= 2.82 for 1:1 magnesium-ofloxacin complex formation, and $\log K_2$= 2.66 for 1:2 complex formation. Therefore major species present in aqueous solutions of **1** and **2** are expected to be free quinolone, Mg^{2+}(aq) ions and Mg:quinolone complexes (1:2, 1:1). The appearance of only one set of resonances in the NMR spectra of the solutions indicates that the exchange between the species is fast on the NMR timescale.

Chemical shifts. The aromatic resonances show only small chemical shift variations between the magnesium-quinolone complexes and the free quinolones. In other studies [17,35] H2 exhibits a characteristic 0.3-0.5 ppm downfield shift upon binding of a divalent metal ion. The small H2 shift observed may be caused by metal-induced stacking, and this shift could be cancelled by an opposite upfield ring current shift which is expected in stacked aromatic quinolones. The result would be a very small net shift, as observed in the spectra.

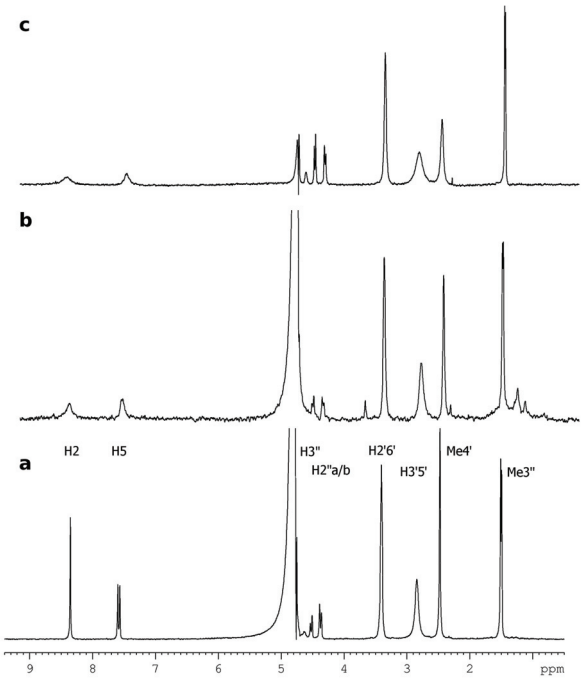

Figure 3. ^{1}H NMR spectra of *S*-ofloxacin (a), complex **1** (b), and complex **2** (c) at 298 K, pH 8.8. All spectra are referenced to the residual HDO resonance at 4.758 ppm.

Line broadening. The most pronounced differences in the NMR spectra between free *S*-ofloxacin and **1** and **2** are the substantial selective line broadening experienced by H2 and H5 in the complexes (Table 3). The inaccuracy of the measurements of line widths at half-height is relatively large due to low signal-to-noise ratio in the spectra. Line broadening of proton signals may be induced by neighbouring paramagnetic metal centres, quadrupolar effects, proton exchange phenomena or decreased tumbling rate due to aggregate formation. Proton exchange and decreased tumbling rate are excluded on the basis that these effects should be observed for all resonances in the complex. Magnesium(II) as diamagnetic nuclei is not

expected to produce paramagnetic line broadening. However, the natural abundance of the quadrupolar ^{25}Mg isotope, spin 5/2 is ~ 10%, and at stoichiometric ratio this could lead to quadrupolar relaxation of adjacent protons.

Table 3. ^{1}H NMR chemical shifts and line widths of the free quinolones and their magnesium complexes.

	Chemical shifts [ppm]		Line widths [Hz]	
	1	**2**	**1**	**2**
H2	8.41 (0.06)	8.43 (0.08)	42.6 (38.5)	82.9 (78.7)
H5	7.56 (-0.02)	7.49 (-0.09)	27.0 (22.8)	46.8 (42.5)
H3´´	n.a. (n.a.)	4.63 (0.00)	n.a. (n.a.)	18.6 (n.a)
H2´´a/ H2´´b	4.53 (0.00)	4.50 (-0.02)	7.9 (1.2)	5.5 (-0.1)
H2´´b/ H2´´a	4.37 (-0.01)	4.34 (-0.03)	7.6 (0.1)	7.8 (2.1)
H2´6´	3.40 (-0.06)	3.38 (-0.02)	12.4 (1.5)	16.1 (5.0)
H3´5´	2.81 (-0.22)	2.84 (0.00)	26.2 (-1.4)	63.8 (39.4)
Me4´	2.45 (-0.18)	2.47 (0.00)	9.9 (1.5)	23.9 (17.5)
Me3´´	1.51 (0.01)	1.47 (-0.03)	6.5 (2.0)	5.2 (0.7)

Differences between free and bound fluoroquinolone given in parenthesis. All shifts are referenced to the residual HDO peak at 4.758 ppm, 298 K. Lines too broad to be measured are designated n.a.

The keto and carboxylate oxygen atoms have previously been identified as the metal ion binding site in 1:1 metal/quinolone complexes by NMR and IR spectroscopy [36]. In order to verify that the binding pattern for complexes **1** and **2** are similar to that of 1:1 complexes, Mn(II) was used as a paramagnetic probe assuming that the two metals have similar coordination geometry. Titration of *S*-ofloxacin was carried out by adding aliquots of $MnCl_2$ solution (FigureS1 in Supplementary Material) [37,38]. The line broadening effect is substantial and only sub-stoichiometric concentration of paramagnetic metal ions was needed to detect interaction. The paramagnetic induced line broadening is seen to be significantly larger for H5 than for H2 (Figure 4, Tables S1 and S2 in Supplementary Material). This is also in agreement with Cu(II) titration data of fluroquinolones [39]. Assuming that the Mn(II) and Mg(II) positions are about equal the difference in line broadening between H2 and H5 agrees qualitatively with the averaged calculated distances in the two crystal structures (Mg(II) - H2 = 5.2 Å; Mg(II) - H5= 4.3 Å). The effect of paramagnetic induced line broadening is proportional to r^6, r being the distance between the metal centre and the proton.

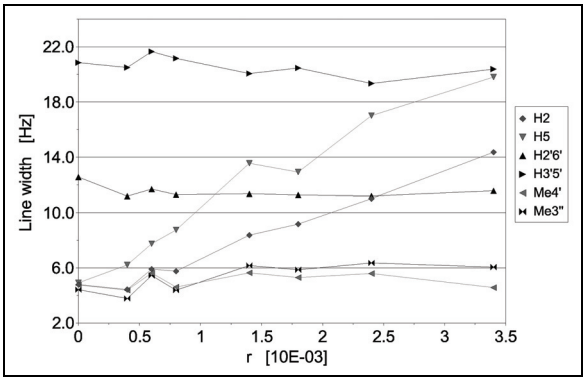

Figure 4. Plot showing the measured line width of the ^{1}H resonances of *S*-ofloxacin with increasing concentration of Mn(II). The ratio ***r*** is given as [Mn(II):*S*-oflo] (times 10^3).

The selective line broadening observed for **1** and **2** is consistent with that expected for keto/carboxyl chelation. However, the relative H2/H5 broadening is seen to be opposite of that observed with paramagnetic probes (Table 3). It is difficult to relate this discrepancy to differences in

coordination chemistry between Mn(II) and Mg(II).

Lecomte and Chenon [40] hypothesised from ^{19}F NMR spectra of the fluoroquinolone pefloxacin that cation binding occurs first at the methylated piperazine nitrogen N4′ and secondly at the keto and carboxyl oxygen atoms. This would be surprising for ofloxacin, taking into account the pK_a values (pKa_1= 6.0, pKa_2= 8.2) and is refuted by the absence of line broadening of the piperazine resonances even at high [Mn(II)]/[ofloxacin] ratios. Sakai et al. [41] have carried out extensive metal binding studies on several fluoroquinolones, however, most of the experiments were performed at pH 2.5, and thus not directly comparable to the present work.

The piperazine resonances of the magnesium-quinolone complexes are severely broadened compared to the free quinolones, as seen in Table 3. The largest effect is on the H3′5′and Me4′ resonances, while the H2′6′ show negligible broadening. The H3′5′ resonances are broad also for the free quinolones due to restricted motion of the piperazine ring, ring inversion and/or slow nitrogen-inversion at the deprotonated N4′ site. For deprotonated N-methyl piperidines, the methyl group favours equatorial position [42], but the free energy difference for equatorial and axial conformation is very low, ca. 2.7 kcal/mol [43] with an anticipated coalescence temperature of 123 K [44]. The induced broadening of the N4′-methyl resonance can therefore only be attributed to a reduced rate of nitrogen pyramidal inversion if there is a direct or indirect interaction to the N4′ site, e.g. through the first or second hydration sphere. This is not the case as even high ratios of Mn(II)/ofloxacin do not show interactions at the N4′ site. The induced broadening may therefore be ascribed to the metal induced aggregation.

We would like to note that also NMR experiments involving titration of a DNA oligonucleotide with complex 1 and 2 have been carried out. However, due to low solubility in water at physiological pH the sensitivity was not high enough to observe any significant effect on the DNA proton signals.

Antimicrobial activity tests and biological relevance of magnesium complexes

The susceptibility of bacteria against tested antibiotics is presented in Table 4.
As already reported [45,46], levofloxacin exerts higher antibacterial activity than ofloxacin. The same trend was observed with magnesium complexes of both antibiotics.

MIC values of **1** and **2** did not significantly differ from those of the non-complexed compounds, showing a general slight decrease in their antibacterial potential. None of the tested compounds showed any special preference for Gram positive or Gram negative bacterial strains. These results are in agreement with results obtained in our previous studies [22,23,24,47,48]. Similar antimicrobial activities of metal complexes and free ligands, as observed in most studies of metal-quinolone complexes are not surprising and are probably due to the intracellular biological conversion of the complexes.

The facts that millimolar concentration of magnesium ion is required for tight binding of quinolones to DNA [49] and that also the interaction between gyrase A and quinolones is enhanced in the presence of magnesium [50] suggest that the interactions between magnesium and quinolone are important for drug activity. The intracellular concentration of

magnesium ions is much higher than that of quinolone [1,36]. According to the stability constants [34] (see NMR discussion) it can be assumed that also in biological systems the mixture of 1:1 and 1:2 magnesium-quinolone complexes, free quinolones, and Mg^{2+}(aq) ions are present. It is probable that magnesium-quinolone complexes and not free quinolones interact with their target DNA-gyrase complex [36,49,51]. On the other hand it is also known that high concentration of extracellular magnesium could antagonize the penetration of fluoroquinolones into the bacterial cell [1].

Table 4. Antibacterial activity of oflo, **1**, *S*-oflo, and **2**. The activity is expressed as MIC (minimal inhibitory concentration, which is the lowest concentration of an antibiotic that will inhibit the growth of a tested organism).

			MIC (μg/ml)	
Microorganism	oflo	**1**	*S*-oflo	**2**
Gram positive:				
Staphylococcus epidermidis	0.75	1	0.3	0.6
Bacillus subtilis	0.5	0.8	0.3	0.5
Micrococcus luteus	12	20	7	10
Gram negative:				
Klebsiella pneumoniae	0.7	1	0.25	0.5
Escherichia coli	0.2	0.25	0.15	0.15
Salmonella enteriditis	0.75	1	0.5	0.75
Pseudomonas aeruginosa	7	10	3	5
Enterococcus faecalis	10	15	4	4

Experimental DNA binding data and computer modeling have shown that four *S*-oflo but only two *R*-oflo molecules can fit the proposed DNA binding site [5]. Evidently, a subtle difference in steric configuration of a nonfunctional group causes a dramatic change in affinity for the receptor site. The computer modeling shows that fitting the enantiomers to DNA is critically dependent on the position of the methyl group at the chiral centre. As realized from the crystal structures the distances between the layers of quinolone rings in **2** are shorter than in **1** and this could be relevant for the number of *S*- and *R*-quinolone molecules bonded at the DNA binding site.

We have found some analogies between our complexes and the magnesium complex of aureolic family drug (chromomycin) and it is appealing to propose that the binding of our complexes to DNA could be similar to the binding of magnesium chromomycin complex [3, 52]. Two chromomycin ligands are coordinated to magnesium through oxygen atoms and octahedral coordination of the metal is completed by two aqua ligands, which is very similar to our complexes **1** and **2**. The crystal structure shows that magnesium complex of chromomycin binds to GGCC

sequence of the octamer`s minor groove. Moreover, the authors have also realized that the stacking of the ligand molecules was more intense in the presence of DNA [52]. Unfortunately our attempts to prepare appropriate crystals and to determine the crystal structure of the magnesium-quinolone complex with DNA were not successful so far.

Conclusions

The stereochemistry of fluoroquinolones is a key factor for the interaction with DNA and gyrase enzymes and the crystal structures of magnesium complexes of ofloxacin enatiomers show that the conformation of the oxazine methyl group influences the crystal packing. In solution, Mg(II) is bound to the keto-carboxylate oxygen atoms, but not to the terminal piperazine nitrogen as shown by Mn(II) titration. The ^{1}H NMR spectra of the solutions containing **1** and **2** exhibit almost identical chemical shift pattern. Both 1:1 and 1:2 Mg:quinolone complexes are present in solution as suggested by the low solubility of **1** and **2**.

Supplementary material is available on request from the authors

Acknowledgments

This work was supported by the Ministry of Higher Education, Science and Technology (MHEST), Republic of Slovenia, project P1-0175 and The Norwegian Research Council, Contract- 145183/V30. The crystallographic data were collected at the Institute for Mineralogy and Crystallography, Geocentre, University of Vienna (compound **1**) and in Ljubljana (compound **2**). PD is grateful to the MHEST, for funding through a junior researcher grant. Special thanks to Prof. B. Čeh and to Prof. J. Sletten for their help. This work is supported by COST Action D20.

References

[1] K. E. Brighty, T. D. Gootz, in: V. T. Andriole (Ed.), The Quinolones, Academic Press, San Diego, 2000, pp. 33-97, and the references therein.
[2] L. A. Mitscher, P. Devasthale, R. Zavod, in: D. C. Hooper, J. S. Wolfson (Eds.), Quinolone Antimicrobial Agents, American Society for Microbiology, Washington DC, 2nd edn., 1993, pp. 3-53.
[3] L.-J. Ming, Med. Res. Rev. 23 (2003) 697-762, and the references therein.
[4] L. L. Shen, A. G. Pernet, Proc. Natl. Acad. Sci. U. S. A 82 (1985) 307-311.
[5] I. Morrissey, K. Hoshino, K. Sato, A. Yoshida, I. Hayakawa, M. G. Bures, L. L. Shen, Antimicrob. Agents Chemother. 40 (1996) 1775-1784.
[6] H. J. Hwangbo, B. H. Yun, J. S. Cha, D. Y. Kwon, S. K. Kim, Eur. J. Pharm. Sci. 18 (2003) 197-203.
[7] I. Turel, Coord. Chem. Rev. 232 (2002) 27-47, and the references therein.

[8] B. Macias, M. V. Villa, I. Rubio, A. Castineiras, J. Borras, J. Inorg. Biochem. 84 (2001) 163-170.
[9] B. Macias, M. V. Villa, M. Sastre, A. Castineiras, J. Borras, J. Pharm. Sci. 91 (2002) 2416-2423.
[10] L. A. Mitscher, Chem. Rev. 105 (2005) 559−592.
[11] C. Sissi, M. Andreolli, V. Cecchetti, A. Fravolini, B. Gatto, M. Palumbo, Bioorg. Med. Chem. 6 (1998) 1555-1561.
[12] M. Palumbo, B. Gatto, G. Zagotto, G. Palu, Trends Microb. 6 (1993) 232-235.
[13] C. G. Noble, F. M. Barnard, A. Maxwell, Antimicrob. Agents Chemother. 47 (2003) 854-862.
[14] B. Llorente, F. Leclerc, R. Cedergren, Bioorg. Med. Chem. 4 (1996) 61-71.
[15] Y. Kwok, Q. Zeng, L. H. Hurley, J. Biol. Chem. 274 (1999) 17226-17235.
[16] I. Turel, I. Leban, M. Zupančič, P. Bukovec, K. Gruber, Acta Cryst. C52 (1996) 2443-2445.
[17] T. Skauge, I. Turel, E. Sletten, Inorg. Chim. Acta 339 (2002) 239-247.
[18] P. Drevenšek, I. Turel, N. Poklar Ulrih, J. Inorg. Biochem. 96 (2003) 407-415.
[19] Z. Otwinowski, W. Minor, Methods Enzymol. 276 (1997) 307-326.
[20] G. M. Sheldrick, SHELX-97, Programs for Crystal Structure Analysis; University of Göttingen: Göttingen, Germany, 1998.
[21] G. Altiokka, Z. Atkosar, N. O. Can, J. Pharm. Biomed. Anal. 30 (2002) 881-885.
[22] I. Turel, A. Šonc, M. Zupančič, K. Sepčič, T. Turk, Metal Based Drugs 7 (2000) 101-104.
[23] P. Drevenšek, A. Golobič, I. Turel, N. Poklar, K. Sepčić, Acta Chim. Slov. 49 (2002) 857-870.
[24] I. Turel, A. Golobič, A. Klavžar, B. Pihlar, P. Buglyó, E. Tolis, D. Rehder, K. Sepčić, J. Inorg. Biochem. 95 (2003) 199-207.
[25] P. Drevenšek, T. Zupančič, B. Pihlar, R. Jerala, U. Kolitsch, A. Plaper, I. Turel, J. Inorg. Biochem. 99 (2005) 432-442.
[26] Y. X. Furet, J. Deshusses, J. C. Pechere, Antimicrob. Agents Chemother. 36 (1992) 2506-2511.
[27] A. G. Orpen, L. Brammer, F. H. Allen, O. Kennard, D. G. Watson, R. Taylor, J. Chem. Soc., Dalton Trans. (1989) S1-S83.
[28] F. H. Allen, O. Kennard, D. G. Watson, L. Brammer, A. G. Orpen, R. Taylor, J. Chem. Soc., Perkin Trans. II (1987) S1-S19.
[29] Z. F. Chen, R. G. Xiong, J. Zhang, X. T. Chen, Z. L. Xue, X. Z. You, Inorg. Chem. 40 (2001) 4075-4077.
[30] Z. R. Qu, H. Zhao, L. X. Xing, X. S. Wang, Z. F. Chen, Z. Yu, R. G. Xiong, X. Z. You, Eur. J. Inorg. Chem. (2003), 2920-2923 and the references therein.
[31] K. Hoshino, K. Sato, K. Akahane, A. Yoshida, I. Hayakawa, M. Sato, T. Une, Y. Osada, Antimicrob. Agents Chemother. 35 (1991) 309-312.
[32] M. Sakai, H. Hara, S. Anjo, M. Nakamura, J. Pharm. Biomed. Anal. 18 (1999) 1057-1067.
[33] A. Mucci, L. Malmusi, M. A. Vandelli, M. Fresta, L. Schenetti, Med. Res. Chem. 6 (1996) 353-363.
[34] J. Shimada, K. Shiba, T. Oguma, H. Miwa, Y. Yoshimura, T. Nishikawa, Y. Okabayashi, T. Kitagawa, S. Yamamoto, Antimicrob. Agents Chemoth. 36 (1992) 1219-1224.

[35] B.M. Sanchez, M.M. Cabarga, A.S. Navarro, A.D.G. Hurle, Int. J. Pharm. 106 (1994) 229-235.
[36] S. Lecomte, M. H. Baron, M. T. Chenon, C. Coupry, N. J. Moreau, Antimicrob. Agents Chemother. 38 (1994) 2810-2816, and the references therein.
[37] G. Navon, G. Valensin, in H. Sigel (Ed.), Metal Ions in Biological Systems, vol. 21, Marcel Dekker, New York, 1987, pp. 1447-1453.
[38] E. Sletten, N. A. Froystein, in H. Sigel (Ed.), Metal Ions in Biological Systems, vol. 32, Marcel Dekker, New York, 1996, pp. 397-418.
[39] I. Turel, J. Košmrlj, B. Andersen, E. Sletten, Metal Based Drugs 6 (1999) 1-4.
[40] S. Lecomte, M. T. Chenon, Int. J. Pharm. 139 (1996) 105-112.
[41] M. Sakai, A. Hara, S. Anjo, M. Nakamura, J. Pharm. Biomed. Anal. 18 (1999) 1057-1067.
[42] I. D. Blackburne, A. R. Katritzky, Y. Takenchi, Acc. Chem. Res. 9 (1975) 300-306.
[43] P. J. Crowley, M. J. T. Robinson, M. G. Ward, Tetrahedron 33 (1977) 915-925.
[44] A. R. Katritzky, R. C. Patel, F. G. Riddell, Angew. Chem. Int. Ed. Engl. 20 (1981) 521-529.
[45] P. Ball, in: V. T. Andriole (Ed.), The Quinolones, Academic Press, San Diego, 2000, pp. 1-31.
[46] R. Stahlmann, H. Lode, in: V. T. Andriole (Ed.), The Quinolones, Academic Press, San Diego, 2000, pp. 397-453.
[47] I. Turel, I. Leban, G. Klintschar, N. Bukovec, S. Zalar, J. Inorg. Biochem. 66 (1997) 77-82.
[48] I. Turel, L. Golič, P. Bukovec, M. Gubina, J. Inorg Biochem. 71 (1998) 53-60.
[49] G. Palu, S. Valisena, G. Ciarocchi, B. Gatto, M. Palumbo, Proc. Natl. Acad. Sci. U. S. A 89 (1992) 9671-9675.
[50] C. Sissi, E. Perdona, E. Domenici, A. Feriani, A. J. Howells, A. Maxwell, M. Palumbo, J. Mol. Biol. 31 (2001) 195-203.
[51] C. J. R. Willmott, A. Maxwell, Antimicrob. Agents Chemother. 37 (1993) 126-127.
[52] M.-H. Hou, H. Robinson, Y.-G. Gao, A. H.-J. Wang, Nucleic Acids Res. 32 (2004) 2214-2222.

Supporting information :

X-Ray Crystallographic, NMR and Antimicrobial Activity Studies of Magnesium Complexes of Fluoroquinolones - Racemic Ofloxacin and Its *S*-form, Levofloxacin.

Petra Drevenšek,[a] Janez Košmrlj,[a] Gerald Giester,[b] Tormod Skauge,[c] Einar Sletten,[c] Kristina Sepčić[d] and Iztok Turel*[a]

Contents:

Table S1. Hydrogen-bonding distances and angles of compound **1,** [Mg(R-oflo)(S-oflo)$(H_2O)_2$]·$2H_2O$ (Å)

D—H· · ·A	D—H	H· · ·A	D· · ·A	D—H· · ·A
O1W—H1W· · ·O12B^{i}	0.76(5)	2.02(5)	2.755(3)	165(4)
O1W—H2W· · ·O11B^{ii}	1.10(5)	1.81(5)	2.894(3)	170(5)
O2W—H3W· · ·O12A^{iii}	0.98(4)	1.80(4)	2.760(3)	165(3)
O2W—H4W· · ·O11A	0.89(4)	1.99(4)	2.868(3)	169(3)
O1M—H11· · ·O12A^{iii}	0.90(3)	1.82(3)	2.710(3)	171(2)
O1M—H12· · ·O2W^{iii}	0.78(4)	1.97(4)	2.719(3)	161(4)
O2M—H21· · ·O1W	1.05(5)	1.68(5)	2.705(3)	165(4)
O2M—H22· · ·O12B^{ii}	0.94(8)	1.82(8)	2.712(3)	158(7)

Symmetry codes: (i) x,y+1,z; (ii) –x,y+½,-z+1; (iii) –x+1,y-½,-z+1

Table S2: Hydrogen-bonding distances and angles of compound **2,** [Mg(S-oflo)$_2$$(H_2O)_2$]·$2H_2O$ (Å)

D—H· · ·A	D—H	H· · ·A	D· · ·A	D—H· ·
O1W—H1W· · ·O12B^{i}	0.99(3)	1.80(3)	2.777(3)	170(3)
O1W—H2W· · ·O11B	0.95(4)	1.89(4)	2.840(3)	177(4)
O2W—H3W· · ·O11A	0.76(4)	2.12(4)	2.872(3)	172(4)
O2W—H4W· · ·O12A^{iii}	1.04(8)	1.81(7)	2.721(4)	144(6)
O1M—H12M· · ·O12B^{i}	1.00(4)	1.72(4)	2.711(3)	171(3)
O1M—H11M· · ·O1W^{i}	0.80(4)	1.99(4)	2.751(4)	160(4)
O2M—H21M· · ·O12A^{ii}	0.79(3)	1.97(3)	2.758(3)	174(4)
O2M—H22M· · ·O2W^{ii}	1.00(5)	1.74(5)	2.676(4)	153(4)

Symmetry codes: (i) –1-x,y-½,-1-z; (ii) –2-x,½+y,-1-z; (iii) –x-2,y,-z-1

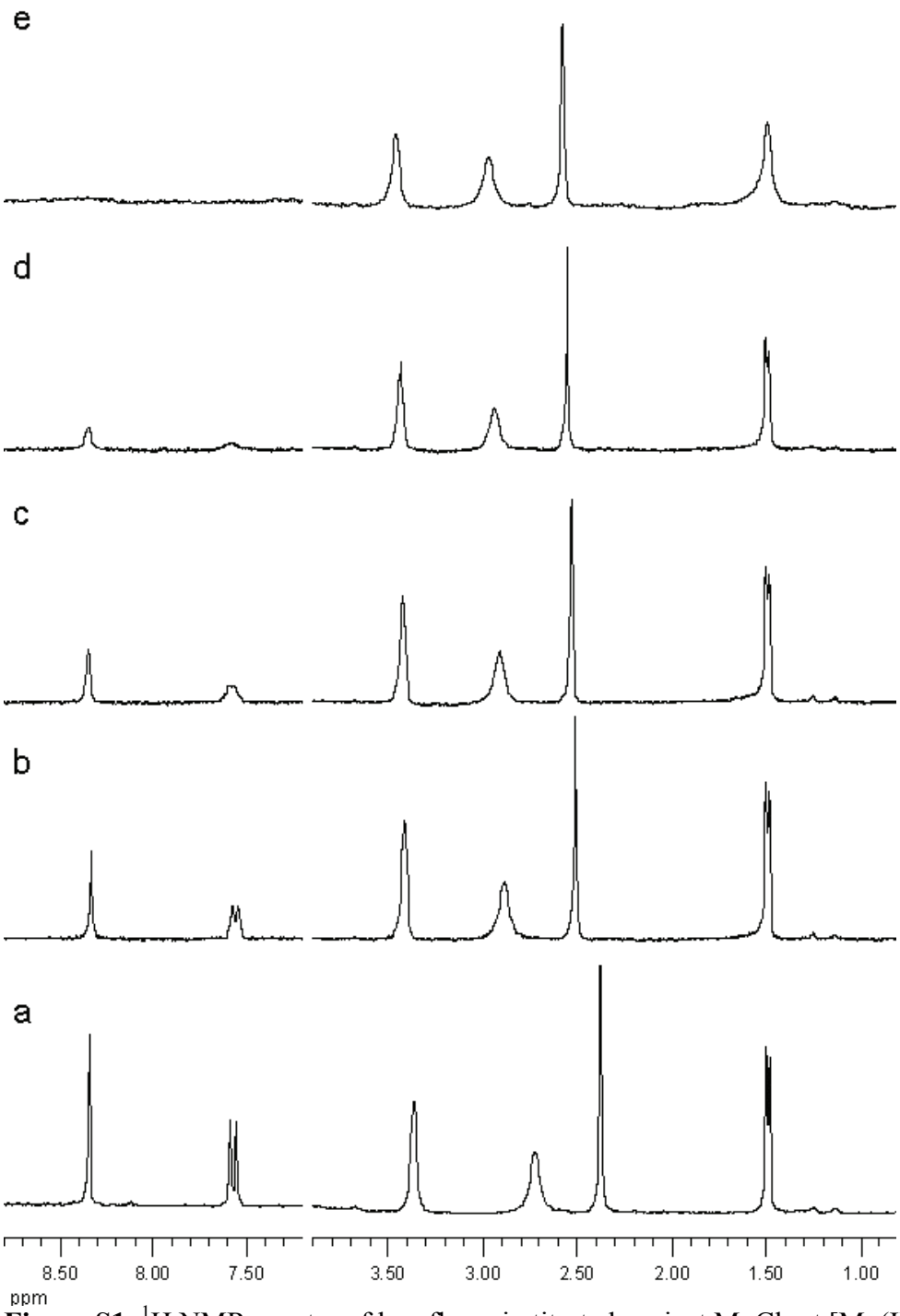

Figure S1. ^{1}H NMR spectra of levofloxacin titrated against $MnCl_2$ at [Mn(II):levofloxacin] ratios (10^{-3}) (from bottom) a) 0.0, b) 0.6, c) 1.4, d) 3.4, e) 16.4. Spectra were recorded at 298K. Chemical shifts in Table S3, line width measurements in Table S4. Note that for reasons of clearity, the vertical scale of the downfield region (8.80-7.20 ppm) is multiplied two times compared to the vertical scale of the upfield region (3.90-0.80 ppm).

Table S3. ^{1}H shifts for Mn(II) titration of levofloxacin.

r	0	0.005	0.03	0.10	0.40	0.60	0.80	1.40	1.80	2.40	3.40	4.40	6.40	16.40
H2	8.34	8.34	8.35	8.35	8.35	8.35	8.35	8.35	8.35	8.35	8.35	8.35	8.34	n.a.
H5	7.57	7.57	7.57	7.57	7.57	7.57	7.58	7.57	7.58	7.58	7.57	7.58	n.a.	n.a.
H2′/H6′	3.37	3.37	3.39	3.41	3.41	3.42	3.42	3.42	3.43	3.43	3.44	3.44	3.45	3.46
H3′/H5′	2.72	2.75	2.81	2.87	2.88	2.89	2.90	2.91	2.92	2.93	2.94	2.95	2.96	2.97
Me4′	2.38	2.40	2.45	2.49	2.51	2.51	2.52	2.53	2.54	2.54	2.55	2.56	2.57	2.58
Me3″	1.49	1.49	1.49	1.49	1.49	1.49	1.49	1.49	1.49	1.49	1.50	1.49	1.50	1.49

The ratio r is given as [Mn(II):levofloxacin] (times 10^3). Some shifts could not be measured due to very broad lines (n.a.).

Table S4. Linewidths for Mn(II) titration of levofloxacin.

r	0	0.005	0.03	0.10	0.40	0.60	0.80	1.40	1.80	2.40	3.40	4.40	6.40	16.40
H2	4.8	3.9	4.7	3.5	4.4	5.9	5.8	8.4	9.2	11.0	14.4	22.8	29.5	n.a.
H5	4.9	4.1	5.0	4.0	6.2	7.8	8.7	13.6	12.9	17.0	19.8	n.a.	n.a.	n.a.
H2′/H6′[a]	12.6	12.0	11.3	10.9	11.2	11.7	11.3	11.4	11.3	11.2	11.6	11.8	12.3	15.3
H3′/H5′[a]	20.9	20.1	19.1	21.2	20.5	21.7	21.2	20.1	20.5	19.3	20.4	22.2	21.2	22.4
Me4′	4.8	4.5	5.3	4.2	4.4	5.6	4.6	5.6	5.3	5.6	4.6	4.8	5.0	6.8
Me3″	4.4	4.3	5.1	3.5	3.8	5.4	4.4	6.2	5.9	6.4	6.1	7.3	8.8	17.9[a]

[a]Due to broad lines, total line width for multiplets was measured.
The ratio r is given as [Mn(II):levofloxacin] (times 10^3).

```
#  CIF produced by WinGX routine CIF_UPDATE
#  Created on 2005-02-17 at 07:50:35
#  Using CIFtbx version 2.6.2 16 Jun 1998

#     CCDC ELECTRONIC DATA DEPOSITION FORM (CIF)

data_global

_publ_contact_author               'Turel, Iztok'
_publ_contact_author_email          iztok.turel@uni-lj.si
_publ_contact_author_address
;
  Faculty of Chemistry and Chemical Technology
  University of Ljubljana
  Askerceva 5
  SI-1001 Ljubljana
  SLOVENIA
;
_publ_contact_author_phone              '+386 1 2419 124'
_publ_contact_author_fax                '+386 1 2419 220'

loop_
_publ_author_name
;
Dreven\<sek, Petra
Ko\<smrlj, Janez
Turel, Iztok
Giester, Gerald
Skauge, Tormod
Sletten, Einar
Sep\<ci\<c, Kristina
;

_journal_name_full
;
Journal of Inorganic Biochemistry
;
_journal_volume
_journal_page_first
_journal_page_last
_journal_year
_ccdc_journal_depnumber


data_cpd1

_audit_creation_date            2005-02-17T07:50:35-00:00
_audit_creation_method         'WinGX routine CIF_UPDATE'

#------------------------------------------------------------------------------#
#                   CHEMICAL INFORMATION                                       #
#------------------------------------------------------------------------------#

_chemical_formula_sum                   'C36 H46 F2 Mg N6 O12'
_chemical_formula_weight                817.1
_chemical_absolute_configuration        syn
_chemical_compound_source               'synthesis as described'

#------------------------------------------------------------------------------#
#                   UNIT CELL INFORMATION                                      #
#------------------------------------------------------------------------------#

_symmetry_cell_setting                  monoclinic
```

```
_symmetry_space_group_name_H-M          P21
loop_
    _symmetry_equiv_pos_as_xyz
'x, y, z'
'-x, y+1/2, -z'

_cell_length_a                          11.0244(3)
_cell_length_b                          9.6181(3)
_cell_length_c                          18.2476(9)
_cell_angle_alpha                       90
_cell_angle_beta                        97.999(3)
_cell_angle_gamma                       90
_cell_volume                            1916.04(12)
_cell_formula_units_Z                   2
_cell_measurement_temperature           200(2)

#-------------------------------------------------------------------------------#
#                   CRYSTAL INFORMATION                                         #
#-------------------------------------------------------------------------------#

_exptl_crystal_description              prism
_exptl_crystal_colour                   yellow
_exptl_crystal_size_max                 0.2
_exptl_crystal_size_mid                 0.17
_exptl_crystal_size_min                 0.1
_exptl_crystal_density_diffrn           1.416
_exptl_crystal_density_method           'not measured'
_exptl_crystal_F_000                    860
_exptl_special_details
;
Nonius KappaCCD difractometer.
8 sets of \w scans. Rotation/frame 2\%.
Crystal-detector distance=30 mm.Measuring time=50 s/\%.
;

#-------------------------------------------------------------------------------#
#                   ABSORPTION CORRECTION                                       #
#-------------------------------------------------------------------------------#

_exptl_absorpt_coefficient_mu           0.127
_exptl_absorpt_correction_type          'multi-scan (Otwinowski & Minor, 1997)'
_exptl_absorpt_correction_T_min         0.975
_exptl_absorpt_correction_T_max         0.987

#-------------------------------------------------------------------------------#
#                   DATA COLLECTION                                             #
#-------------------------------------------------------------------------------#

_diffrn_ambient_temperature             200(2)
_diffrn_radiation_wavelength            0.71073
_diffrn_radiation_probe                 x-ray
_diffrn_radiation_type                  MoK\a
_diffrn_radiation_monochromator         graphite
_diffrn_radiation_source                'fine-focus seald tube'
_diffrn_measurement_device_type         'Nonius KappaCCD diffractometer'
_diffrn_measurement_method
;
\w scans
;
_diffrn_reflns_av_R_equivalents         0.0207
_diffrn_reflns_av_unetI/netI            0.0338
_diffrn_reflns_number                   15160
_diffrn_reflns_limit_h_min              -13
_diffrn_reflns_limit_h_max              13
```

```
_diffrn_reflns_limit_k_min              -12
_diffrn_reflns_limit_k_max              12
_diffrn_reflns_limit_l_min              -22
_diffrn_reflns_limit_l_max              22
_diffrn_reflns_theta_min                3.45
_diffrn_reflns_theta_max                26.37
_diffrn_reflns_theta_full               26.37
_diffrn_measured_fraction_theta_full    0.994
_diffrn_measured_fraction_theta_max     0.994
_reflns_number_total                    7804
_reflns_number_gt                       6624
_reflns_threshold_expression            >2sigma(I)

#---------------------------------------------------------------------------#
#                   COMPUTER PROGRAMS USED                                  #
#---------------------------------------------------------------------------#

_computing_data_collection
;
COLLECT (Nonius, 1999)
;
_computing_cell_refinement
;
DENZO and SCALEPACK (Otwinowski & Minor, 1997)
;
_computing_data_reduction
;
DENZO and SCALEPACK (Otwinowski & Minor, 1997)
;
_computing_structure_solution           'SHELXS-97 (Sheldrick, 1997)'
_computing_structure_refinement         'SHELXL-97 (Sheldrick, 1997)'
_computing_molecular_graphics
;
PLUTON (Spek, 1991),
PLATON (Spek, 2003),
ORTEP-3 (Farrugia, 1999)
MERCURY (Bruno et al., 2002)
;
_computing_publication_material
;
WinGX publication routines (Farrugia, 1999)'
;

#---------------------------------------------------------------------------#
#                   REFINEMENT INFORMATION                                  #
#---------------------------------------------------------------------------#

_refine_special_details
;
 Refinement of F^2^ against ALL reflections.  The weighted R-factor wR and
 goodness of fit S are based on F^2^, conventional R-factors R are based
 on F, with F set to zero for negative F^2^. The threshold expression of
 F^2^ > 2sigma(F^2^) is used only for calculating R-factors(gt) etc. and is
 not relevant to the choice of reflections for refinement.  R-factors based
 on F^2^ are statistically about twice as large as those based on F, and R-
 factors based on ALL data will be even larger.
;
_refine_ls_structure_factor_coef        Fsqd
_refine_ls_matrix_type                  full
_refine_ls_weighting_scheme             calc
_refine_ls_weighting_details
         'calc w=1/[\s^2^(Fo^2^)+(0.0596P)^2^+0.9314P] where P=(Fo^2^+2Fc^2^)/3'
_atom_sites_solution_primary            direct
_atom_sites_solution_secondary          difmap
```

```
_atom_sites_solution_hydrogens          difmap
_refine_ls_hydrogen_treatment           refall
_refine_ls_extinction_method            SHELXL97
_refine_ls_extinction_expression
                                    Fc^*^=kFc[1+0.001xFc^2^\l^3^/sin(2\q)]^-1/4^
_refine_ls_extinction_coef              0.0068(11)
_refine_ls_number_reflns                7804
_refine_ls_number_parameters            547
_refine_ls_number_restraints            1
_refine_ls_R_factor_all                 0.0565
_refine_ls_R_factor_gt                  0.0459
_refine_ls_wR_factor_ref                0.1206
_refine_ls_wR_factor_gt                 0.1137
_refine_ls_goodness_of_fit_ref          1.019
_refine_ls_restrained_S_all             1.019
_refine_ls_shift/su_max                 0.019
_refine_ls_shift/su_mean                0.004
_refine_ls_abs_structure_details        'Flack (1983), Acta Cryst. A39, 876-881'
_refine_ls_abs_structure_Flack          0.3(4)
_refine_diff_density_max                0.926
_refine_diff_density_min                -0.388
_refine_diff_density_rms                0.052

#-----------------------------------------------------------------------------#
#                   ATOMIC TYPES, COORDINATES AND THERMAL PARAMETERS          #
#-----------------------------------------------------------------------------#

loop_
    _atom_type_symbol
    _atom_type_description
    _atom_type_scat_dispersion_real
    _atom_type_scat_dispersion_imag
    _atom_type_scat_source
C C 0.0033 0.0016 'International Tables Vol C Tables 4.2.6.8 and 6.1.1.4'
H H 0 0 'International Tables Vol C Tables 4.2.6.8 and 6.1.1.4'
F F 0.0171 0.0103 'International Tables Vol C Tables 4.2.6.8 and 6.1.1.4'
Mg Mg 0.0486 0.0363 'International Tables Vol C Tables 4.2.6.8 and 6.1.1.4'
N N 0.0061 0.0033 'International Tables Vol C Tables 4.2.6.8 and 6.1.1.4'
O O 0.0106 0.006 'International Tables Vol C Tables 4.2.6.8 and 6.1.1.4'

loop_
 _atom_site_label
 _atom_site_type_symbol
 _atom_site_fract_x
 _atom_site_fract_y
 _atom_site_fract_z
 _atom_site_U_iso_or_equiv
 _atom_site_adp_type
 _atom_site_occupancy
 _atom_site_symmetry_multiplicity
 _atom_site_calc_flag
 _atom_site_refinement_flags
 _atom_site_disorder_assembly
 _atom_site_disorder_group
Mg Mg 0.24716(10) 0.31216(13) 0.50019(6) 0.02297(16) Uani 1 1 d . . .
F1A F -0.01420(17) 0.3133(2) 0.81938(9) 0.0385(4) Uani 1 1 d . . .
O1A O 0.21149(19) 0.3648(2) 0.60342(11) 0.0283(5) Uani 1 1 d . . .
O11A O 0.33140(18) 0.4992(2) 0.49559(10) 0.0288(5) Uani 1 1 d . . .
O12A O 0.3874(2) 0.7154(2) 0.52607(12) 0.0353(5) Uani 1 1 d . . .
O2A O 0.0130(2) 0.8018(2) 0.79049(11) 0.0355(5) Uani 1 1 d . . .
N1A N 0.1498(3) 0.7592(3) 0.67401(15) 0.0358(6) Uani 1 1 d . . .
N21A N -0.0523(2) 0.5673(3) 0.87468(13) 0.0292(6) Uani 1 1 d . . .
N24A N -0.1812(2) 0.6046(3) 0.99751(13) 0.0366(6) Uani 1 1 d . . .
C1A C 0.3277(3) 0.6073(3) 0.53442(16) 0.0260(6) Uani 1 1 d . . .
```

```
C2A C 0.2184(3) 0.7373(3) 0.62044(18) 0.0359(8) Uani 1 1 d . . .
H2A H 0.2500 0.8150 0.5994 0.043 Uiso 1 1 calc R . .
C3A C 0.2459(3) 0.6100(3) 0.59396(16) 0.0271(6) Uani 1 1 d . . .
C4A C 0.1961(3) 0.4879(3) 0.62405(15) 0.0238(6) Uani 1 1 d . . .
C5A C 0.0802(3) 0.3990(3) 0.72145(16) 0.0274(6) Uani 1 1 d . . .
H5A H 0.0896 0.3088 0.7048 0.033 Uiso 1 1 calc R . .
C6A C 0.0228(3) 0.4232(3) 0.78149(16) 0.0277(7) Uani 1 1 d . . .
C7A C 0.0001(3) 0.5572(3) 0.80883(17) 0.0262(6) Uani 1 1 d . . .
C8A C 0.0375(3) 0.6689(3) 0.76879(16) 0.0273(6) Uani 1 1 d . . .
C9A C 0.1043(3) 0.6468(3) 0.70941(15) 0.0254(6) Uani 1 1 d . . .
C10A C 0.1251(3) 0.5124(3) 0.68510(15) 0.0232(6) Uani 1 1 d . . .
C12A C 0.1263(4) 0.9023(4) 0.6984(3) 0.0570(12) Uani 1 1 d . . .
H12A H 0.1132 0.9601 0.6538 0.068 Uiso 1 1 calc R . .
C11A C 0.0082(4) 0.9006(4) 0.7298(2) 0.0486(9) Uani 1 1 d . . .
H11A H -0.0084 0.9929 0.7475 0.058 Uiso 1 1 calc R . .
H11B H -0.0580 0.8757 0.6914 0.058 Uiso 1 1 calc R . .
C13A C 0.2284(4) 0.9588(5) 0.7445(3) 0.0723(14) Uani 1 1 d . . .
H13A H 0.2991 0.9555 0.7192 0.108 Uiso 1 1 calc R . .
H13B H 0.2438 0.9056 0.7893 0.108 Uiso 1 1 calc R . .
H13C H 0.2115 1.0535 0.7562 0.108 Uiso 1 1 calc R . .
C14A C -0.2075(4) 0.5655(4) 1.07131(19) 0.0497(9) Uani 1 1 d . . .
H14A H -0.1883 0.6419 1.1048 0.075 Uiso 1 1 calc R . .
H14B H -0.1588 0.4863 1.0887 0.075 Uiso 1 1 calc R . .
H14C H -0.2928 0.5427 1.0688 0.075 Uiso 1 1 calc R . .
C22A C -0.1816(2) 0.5280(3) 0.87000(15) 0.0344(6) Uani 1 1 d . . .
H22A H -0.1985 0.4495 0.8368 0.041 Uiso 1 1 calc R . .
H22B H -0.2329 0.6051 0.8503 0.041 Uiso 1 1 calc R . .
C23A C -0.2105(3) 0.4900(3) 0.94581(16) 0.0408(7) Uani 1 1 d . . .
H23A H -0.2968 0.4674 0.9428 0.049 Uiso 1 1 calc R . .
H23B H -0.1637 0.4085 0.9637 0.049 Uiso 1 1 calc R . .
C25A C -0.0522(3) 0.6415(4) 1.00101(15) 0.0440(7) Uani 1 1 d . . .
H25A H -0.0020 0.5627 1.0194 0.053 Uiso 1 1 calc R . .
H25B H -0.0335 0.7179 1.0354 0.053 Uiso 1 1 calc R . .
C26A C -0.0214(3) 0.6833(4) 0.92564(15) 0.0425(7) Uani 1 1 d . . .
H26A H -0.0679 0.7652 0.9080 0.051 Uiso 1 1 calc R . .
H26B H 0.0651 0.7049 0.9289 0.051 Uiso 1 1 calc R . .
F1B F 0.51201(19) 0.3294(2) 0.18536(10) 0.0436(5) Uani 1 1 d . . .
O1B O 0.28297(19) 0.2613(2) 0.39687(11) 0.0285(5) Uani 1 1 d . . .
O11B O 0.16601(17) 0.1224(2) 0.50428(11) 0.0279(4) Uani 1 1 d . . .
O12B O 0.1201(2) -0.0966(2) 0.47528(13) 0.0385(6) Uani 1 1 d . . .
O2B O 0.4864(2) -0.1624(2) 0.20541(12) 0.0373(5) Uani 1 1 d . . .
N1B N 0.3582(2) -0.1288(3) 0.32615(14) 0.0296(6) Uani 1 1 d . . .
N21B N 0.5526(2) 0.0618(3) 0.12597(14) 0.0320(6) Uani 1 1 d . . .
N24B N 0.6924(3) 0.0542(3) 0.00640(15) 0.0433(8) Uani 1 1 d . . .
C1B C 0.1751(3) 0.0141(3) 0.46562(15) 0.0242(6) Uani 1 1 d . . .
C2B C 0.2889(3) -0.1117(3) 0.38071(16) 0.0275(6) Uani 1 1 d . . .
H2B H 0.2606 -0.1909 0.4022 0.033 Uiso 1 1 calc R . .
C3B C 0.2574(3) 0.0164(3) 0.40673(16) 0.0249(6) Uani 1 1 d . . .
C4B C 0.3011(3) 0.1405(3) 0.37572(15) 0.0237(6) Uani 1 1 d . . .
C5B C 0.4109(3) 0.2357(3) 0.27715(15) 0.0285(7) Uani 1 1 d . . .
H5B H 0.3959 0.3255 0.2926 0.034 Uiso 1 1 calc R . .
C6B C 0.4724(3) 0.2138(3) 0.21846(16) 0.0298(7) Uani 1 1 d . . .
C7B C 0.4984(3) 0.0833(3) 0.19034(17) 0.0282(7) Uani 1 1 d . . .
C8B C 0.4636(3) -0.0316(3) 0.22938(15) 0.0273(7) Uani 1 1 d . . .
C9B C 0.3987(3) -0.0134(3) 0.29066(15) 0.0262(6) Uani 1 1 d . . .
C10B C 0.3707(3) 0.1204(3) 0.31371(16) 0.0251(6) Uani 1 1 d . . .
C11B C 0.4993(3) -0.2629(4) 0.26486(19) 0.0442(9) Uani 1 1 d . . .
H11C H 0.5693 -0.2380 0.3007 0.053 Uiso 1 1 calc R . .
H11D H 0.5152 -0.3536 0.2450 0.053 Uiso 1 1 calc R . .
C12B C 0.3880(3) -0.2717(3) 0.30328(16) 0.0340(8) Uani 1 1 d . . .
H12B H 0.4066 -0.3300 0.3475 0.041 Uiso 1 1 calc R . .
C13B C 0.2774(3) -0.3324(4) 0.25368(17) 0.0469(9) Uani 1 1 d . . .
H13D H 0.2086 -0.3362 0.2806 0.070 Uiso 1 1 calc R . .
H13E H 0.2966 -0.4244 0.2385 0.070 Uiso 1 1 calc R . .
```

```
H13F H 0.2577 -0.2745 0.2108 0.070 Uiso 1 1 calc R . .
C14B C 0.7254(3) 0.0015(5) -0.06300(18) 0.0556(10) Uani 1 1 d . . .
H14D H 0.8088 -0.0301 -0.0553 0.083 Uiso 1 1 calc R . .
H14E H 0.7168 0.0744 -0.0993 0.083 Uiso 1 1 calc R . .
H14F H 0.6724 -0.0744 -0.0801 0.083 Uiso 1 1 calc R . .
C22B C 0.5346(3) 0.1663(4) 0.06684(15) 0.0474(8) Uani 1 1 d . . .
H22C H 0.5864 0.2463 0.0805 0.057 Uiso 1 1 calc R . .
H22D H 0.4500 0.1971 0.0595 0.057 Uiso 1 1 calc R . .
C23B C 0.5667(3) 0.1032(4) -0.00388(17) 0.0480(8) Uani 1 1 d . . .
H23C H 0.5120 0.0261 -0.0187 0.058 Uiso 1 1 calc R . .
H23D H 0.5560 0.1722 -0.0430 0.058 Uiso 1 1 calc R . .
C25B C 0.7073(3) -0.0522(4) 0.06328(16) 0.0439(7) Uani 1 1 d . . .
H25C H 0.7912 -0.0854 0.0701 0.053 Uiso 1 1 calc R . .
H25D H 0.6541 -0.1302 0.0478 0.053 Uiso 1 1 calc R . .
C26B C 0.6762(2) 0.0051(4) 0.13573(15) 0.0409(7) Uani 1 1 d . . .
H26C H 0.6826 -0.0685 0.1725 0.049 Uiso 1 1 calc R . .
H26D H 0.7342 0.0774 0.1535 0.049 Uiso 1 1 calc R . .
O1M O 0.41351(19) 0.2239(2) 0.54578(13) 0.0302(5) Uani 1 1 d . . .
O2M O 0.0824(2) 0.4010(2) 0.45561(12) 0.0323(5) Uani 1 1 d . . .
O1W O 0.0290(2) 0.6625(3) 0.40682(13) 0.0349(5) Uani 1 1 d . . .
O2W O 0.5259(2) 0.4610(2) 0.40816(12) 0.0342(5) Uani 1 1 d . . .
H11M H 0.482(2) 0.229(3) 0.5247(12) 0.012(6) Uiso 1 1 d . . .
H12M H 0.413(3) 0.146(5) 0.559(2) 0.044(11) Uiso 1 1 d . . .
H21M H 0.078(4) 0.503(6) 0.435(2) 0.069(13) Uiso 1 1 d . . .
H22M H 0.003(8) 0.408(9) 0.467(4) 0.19(3) Uiso 1 1 d . . .
H1W H 0.052(4) 0.733(5) 0.418(2) 0.055(13) Uiso 1 1 d . . .
H2W H -0.044(5) 0.635(7) 0.440(3) 0.114(19) Uiso 1 1 d . . .
H3W H 0.571(3) 0.382(4) 0.4339(19) 0.045(10) Uiso 1 1 d . . .
H4W H 0.460(3) 0.466(4) 0.4302(19) 0.048(10) Uiso 1 1 d . . .

loop_
 _atom_site_aniso_label
 _atom_site_aniso_U_11
 _atom_site_aniso_U_22
 _atom_site_aniso_U_33
 _atom_site_aniso_U_23
 _atom_site_aniso_U_13
 _atom_site_aniso_U_12
Mg 0.0254(3) 0.0194(3) 0.0259(3) -0.0028(2) 0.0099(3) -0.0005(3)
F1A 0.0508(10) 0.0329(10) 0.0357(9) 0.0033(8) 0.0199(8) -0.0065(9)
O1A 0.0366(11) 0.0217(11) 0.0292(11) -0.0046(9) 0.0138(9) -0.0012(9)
O11A 0.0340(11) 0.0251(11) 0.0303(10) -0.0079(9) 0.0156(8) -0.0040(9)
O12A 0.0409(12) 0.0239(11) 0.0461(13) -0.0072(10) 0.0230(11) -0.0091(10)
O2A 0.0437(12) 0.0325(12) 0.0335(12) -0.0040(10) 0.0167(10) 0.0073(10)
N1A 0.0499(16) 0.0232(13) 0.0396(15) -0.0037(12) 0.0251(13) -0.0012(12)
N21A 0.0258(13) 0.0413(17) 0.0219(13) -0.0055(11) 0.0084(10) -0.0040(11)
N24A 0.0352(13) 0.0510(16) 0.0261(12) 0.0021(11) 0.0137(10) 0.0059(12)
C1A 0.0264(14) 0.0207(14) 0.0326(15) -0.0015(13) 0.0107(11) 0.0010(13)
C2A 0.0439(19) 0.0241(17) 0.0452(19) -0.0022(15) 0.0253(15) -0.0052(14)
C3A 0.0286(14) 0.0255(15) 0.0291(15) -0.0034(14) 0.0101(12) -0.0012(13)
C4A 0.0239(13) 0.0205(15) 0.0274(14) -0.0005(12) 0.0053(11) -0.0001(12)
C5A 0.0287(14) 0.0268(16) 0.0275(15) -0.0034(12) 0.0073(12) -0.0025(12)
C6A 0.0282(15) 0.0307(17) 0.0251(14) 0.0011(13) 0.0063(12) -0.0049(13)
C7A 0.0252(14) 0.0325(16) 0.0220(14) -0.0045(11) 0.0073(12) 0.0009(12)
C8A 0.0265(14) 0.0306(17) 0.0258(14) -0.0044(13) 0.0073(11) 0.0030(12)
C9A 0.0238(14) 0.0253(16) 0.0274(14) 0.0004(13) 0.0051(11) 0.0001(12)
C10A 0.0257(14) 0.0251(15) 0.0186(13) -0.0008(12) 0.0028(10) -0.0004(13)
C12A 0.076(3) 0.0230(18) 0.085(3) -0.0174(18) 0.056(2) -0.0076(17)
C11A 0.067(2) 0.0328(19) 0.053(2) 0.0012(16) 0.0318(19) 0.0123(17)
C13A 0.056(2) 0.066(3) 0.097(3) -0.037(3) 0.018(2) 0.007(2)
C14A 0.055(2) 0.065(2) 0.0326(16) 0.0065(15) 0.0184(15) 0.0046(17)
C22A 0.0267(13) 0.0474(17) 0.0295(13) -0.0029(12) 0.0053(11) -0.0036(13)
C23A 0.0353(15) 0.0504(18) 0.0392(15) 0.0014(14) 0.0143(12) -0.0030(14)
C25A 0.0425(16) 0.062(2) 0.0290(14) -0.0129(14) 0.0123(12) -0.0047(15)
```

```
C26A 0.0401(16) 0.0569(19) 0.0328(14) -0.0153(13) 0.0132(12) -0.0140(14)
F1B 0.0601(12) 0.0370(11) 0.0384(10) -0.0012(9) 0.0242(9) -0.0112(9)
O1B 0.0391(12) 0.0197(11) 0.0293(11) -0.0019(8) 0.0138(9) -0.0001(9)
O11B 0.0301(10) 0.0222(10) 0.0342(11) -0.0043(9) 0.0139(8) -0.0039(9)
O12B 0.0421(13) 0.0268(12) 0.0520(14) -0.0071(10) 0.0258(11) -0.0098(10)
O2B 0.0514(13) 0.0304(12) 0.0328(12) -0.0033(10) 0.0153(10) 0.0119(10)
N1B 0.0356(13) 0.0222(13) 0.0326(13) -0.0057(11) 0.0110(11) 0.0036(11)
N21B 0.0273(13) 0.0454(18) 0.0240(13) 0.0006(11) 0.0061(11) 0.0056(12)
N24B 0.0388(15) 0.062(2) 0.0319(14) -0.0038(12) 0.0150(12) -0.0040(13)
C1B 0.0245(13) 0.0222(15) 0.0268(14) -0.0015(13) 0.0066(11) -0.0031(13)
C2B 0.0326(15) 0.0234(16) 0.0275(15) -0.0040(12) 0.0078(12) -0.0017(12)
C3B 0.0247(14) 0.0222(15) 0.0288(15) -0.0027(13) 0.0078(11) -0.0008(13)
C4B 0.0251(13) 0.0258(17) 0.0203(13) -0.0035(12) 0.0033(11) 0.0016(12)
C5B 0.0361(16) 0.0260(17) 0.0241(14) -0.0015(12) 0.0066(12) -0.0025(13)
C6B 0.0342(16) 0.0317(17) 0.0245(14) -0.0003(13) 0.0079(12) -0.0063(14)
C7B 0.0211(14) 0.0408(19) 0.0225(14) -0.0012(13) 0.0028(11) 0.0011(12)
C8B 0.0271(14) 0.0313(17) 0.0236(14) -0.0049(12) 0.0037(12) 0.0050(12)
C9B 0.0297(15) 0.0274(16) 0.0228(13) -0.0028(12) 0.0079(11) 0.0028(13)
C10B 0.0241(14) 0.0256(15) 0.0261(14) -0.0044(13) 0.0052(11) -0.0005(13)
C11B 0.062(2) 0.0319(19) 0.0437(18) -0.0002(15) 0.0239(17) 0.0179(16)
C12B 0.0425(18) 0.0295(17) 0.0271(15) 0.0003(12) -0.0049(13) 0.0129(14)
C13B 0.067(2) 0.039(2) 0.0336(17) -0.0036(15) 0.0047(16) 0.0063(18)
C14B 0.056(2) 0.078(3) 0.0384(17) -0.0102(19) 0.0246(15) -0.008(2)
C22B 0.0556(19) 0.057(2) 0.0320(15) 0.0069(14) 0.0152(13) 0.0146(16)
C23B 0.0527(19) 0.062(2) 0.0316(15) 0.0056(15) 0.0146(13) 0.0072(17)
C25B 0.0316(14) 0.064(2) 0.0373(15) -0.0046(15) 0.0090(12) 0.0078(14)
C26B 0.0267(14) 0.068(2) 0.0286(14) -0.0037(15) 0.0046(11) 0.0099(15)
O1M 0.0236(11) 0.0300(13) 0.0389(12) 0.0060(10) 0.0106(9) 0.0027(9)
O2M 0.0309(11) 0.0296(12) 0.0385(12) 0.0068(10) 0.0118(10) 0.0044(10)
O1W 0.0374(13) 0.0236(12) 0.0459(13) -0.0042(11) 0.0131(10) 0.0002(10)
O2W 0.0369(12) 0.0239(12) 0.0437(13) 0.0020(10) 0.0122(10) -0.0021(10)


_geom_special_details
;
 All esds (except the esd in the dihedral angle between two l.s. planes)
 are estimated using the full covariance matrix.  The cell esds are taken
 into account individually in the estimation of esds in distances, angles
 and torsion angles; correlations between esds in cell parameters are only
 used when they are defined by crystal symmetry.  An approximate (isotropic)
 treatment of cell esds is used for estimating esds involving l.s. planes.
;

loop_
 _geom_bond_atom_site_label_1
 _geom_bond_atom_site_label_2
 _geom_bond_distance
 _geom_bond_site_symmetry_2
 _geom_bond_publ_flag
Mg O11A 2.032(2) .
Mg O11B 2.038(2) .
Mg O1B 2.039(2) .
Mg O1A 2.041(2) .
Mg O2M 2.069(2) .
Mg O1M 2.086(2) .
F1A C6A 1.356(4) .
O1A C4A 1.261(4) .
O11A C1A 1.262(4) .
O12A C1A 1.251(4) .
O2A C8A 1.376(4) .
O2A C11A 1.454(4) .
N1A C2A 1.333(4) .
N1A C9A 1.388(4) .
N1A C12A 1.481(4) .
N21A C7A 1.407(4) .
N21A C26A 1.462(4) .
N21A C22A 1.465(4) .
N24A C23A 1.457(4) .
N24A C25A 1.458(4) .
N24A C14A 1.466(4) .
C1A C3A 1.506(4) .
C2A C3A 1.366(5) .
C2A H2A 0.9300 .
C3A C4A 1.437(4) .
C4A C10A 1.467(4) .
C5A C6A 1.359(4) .
C5A C10A 1.402(4) .
C5A H5A 0.9300 .
C6A C7A 1.417(4) .
C7A C8A 1.394(4) .
C8A C9A 1.408(4) .
C9A C10A 1.397(5) .
C12A C13A 1.416(6) .
C12A C11A 1.494(5) .
C12A H12A 0.9800 .
```

```
C11A H11A 0.9700 .
C11A H11B 0.9700 .
C13A H13A 0.9600 .
C13A H13B 0.9600 .
C13A H13C 0.9600 .
C14A H14A 0.9600 .
C14A H14B 0.9600 .
C14A H14C 0.9600 .
C22A C23A 1.507(4) .
C22A H22A 0.9700 .
C22A H22B 0.9700 .
C23A H23A 0.9700 .
C23A H23B 0.9700 .
C25A C26A 1.516(4) .
C25A H25A 0.9700 .
C25A H25B 0.9700 .
C26A H26A 0.9700 .
C26A H26B 0.9700 .
F1B C6B 1.366(4) .
O1B C4B 1.249(4) .
O11B C1B 1.270(4) .
O12B C1B 1.250(4) .
O2B C8B 1.366(4) .
O2B C11B 1.445(4) .
N1B C2B 1.346(4) .
N1B C9B 1.390(4) .
N1B C12B 1.487(4) .
N21B C7B 1.405(4) .
N21B C26B 1.455(4) .
N21B C22B 1.468(4) .
N24B C23B 1.451(4) .
N24B C25B 1.451(4) .
N24B C14B 1.456(4) .
C1B C3B 1.500(4) .
C2B C3B 1.382(4) .
C2B H2B 0.9300 .
C3B C4B 1.433(4) .
C4B C10B 1.465(4) .
C5B C6B 1.361(4) .
C5B C10B 1.398(4) .
C5B H5B 0.9300 .
C6B C7B 1.401(5) .
C7B C8B 1.397(4) .
C8B C9B 1.420(4) .
C9B C10B 1.401(4) .
C11B C12B 1.498(5) .
C11B H11C 0.9700 .
C11B H11D 0.9700 .
C12B C13B 1.529(5) .
C12B H12B 0.9800 .
C13B H13D 0.9600 .
C13B H13E 0.9600 .
C13B H13F 0.9600 .
C14B H14D 0.9600 .
C14B H14E 0.9600 .
C14B H14F 0.9600 .
C22B C23B 1.512(4) .
C22B H22C 0.9700 .
C22B H22D 0.9700 .
C23B H23C 0.9700 .
C23B H23D 0.9700 .
C25B C26B 1.515(4) .
C25B H25C 0.9700 .
C25B H25D 0.9700 .
C26B H26C 0.9700 .
C26B H26D 0.9700 .
O1M H11M 0.89(3) .
O1M H12M 0.79(4) .
O2M H21M 1.05(5) .
O2M H22M 0.93(8) .
O1W H1W 0.75(5) .
O1W H2W 1.10(5) .
O2W H3W 0.99(4) .
O2W H4W 0.88(4) .

loop_
 _geom_angle_atom_site_label_1
 _geom_angle_atom_site_label_2
 _geom_angle_atom_site_label_3
 _geom_angle
 _geom_angle_site_symmetry_1
 _geom_angle_site_symmetry_3
 _geom_angle_publ_flag
O11A Mg O11B 178.76(11) . .
O11A Mg O1B 91.48(9) . .
O11B Mg O1B 87.79(9) . .
O11A Mg O1A 88.08(9) . .
O11B Mg O1A 92.65(9) . .
O1B Mg O1A 179.53(13) . .
O11A Mg O2M 89.97(10) . .
O11B Mg O2M 91.05(9) . .
O1B Mg O2M 90.46(10) . .
O1A Mg O2M 89.37(10) . .
O11A Mg O1M 89.73(10) . .
O11B Mg O1M 89.27(10) . .
O1B Mg O1M 89.91(10) . .
O1A Mg O1M 90.26(10) . .
O2M Mg O1M 179.52(14) . .
C4A O1A Mg 124.02(19) . .
C1A O11A Mg 130.96(18) . .
C8A O2A C11A 112.1(2) . .
C2A N1A C9A 119.8(3) . .
C2A N1A C12A 120.5(3) . .
C9A N1A C12A 119.6(2) . .
C7A N21A C26A 120.6(2) . .
C7A N21A C22A 116.4(2) . .
C26A N21A C22A 111.8(2) . .
C23A N24A C25A 109.8(2) . .
C23A N24A C14A 110.3(3) . .
C25A N24A C14A 109.8(3) . .
O12A C1A O11A 123.9(2) . .
O12A C1A C3A 116.9(3) . .
O11A C1A C3A 119.3(3) . .
N1A C2A C3A 125.3(3) . .
N1A C2A H2A 117.4 . .
C3A C2A H2A 117.4 . .
C2A C3A C4A 118.8(2) . .
C2A C3A C1A 117.1(3) . .
C4A C3A C1A 124.1(3) . .
O1A C4A C3A 125.4(3) . .
O1A C4A C10A 119.0(2) . .
C3A C4A C10A 115.6(3) . .
C6A C5A C10A 118.9(3) . .
C6A C5A H5A 120.6 . .
C10A C5A H5A 120.6 . .
F1A C6A C5A 119.0(3) . .
F1A C6A C7A 116.7(2) . .
C5A C6A C7A 124.3(3) . .
```

```
C8A C7A N21A 125.6(3) . .
C8A C7A C6A 115.9(3) . .
N21A C7A C6A 118.5(3) . .
O2A C8A C7A 118.7(2) . .
O2A C8A C9A 120.4(3) . .
C7A C8A C9A 120.8(3) . .
N1A C9A C10A 119.1(2) . .
N1A C9A C8A 120.2(3) . .
C10A C9A C8A 120.7(3) . .
C9A C10A C5A 119.0(3) . .
C9A C10A C4A 121.2(3) . .
C5A C10A C4A 119.7(3) . .
C13A C12A N1A 112.1(4) . .
C13A C12A C11A 116.0(4) . .
N1A C12A C11A 107.7(3) . .
C13A C12A H12A 106.8 . .
N1A C12A H12A 106.8 . .
C11A C12A H12A 106.8 . .
O2A C11A C12A 111.0(3) . .
O2A C11A H11A 109.4 . .
C12A C11A H11A 109.4 . .
O2A C11A H11B 109.4 . .
C12A C11A H11B 109.4 . .
H11A C11A H11B 108.0 . .
C12A C13A H13A 109.5 . .
C12A C13A H13B 109.5 . .
H13A C13A H13B 109.5 . .
C12A C13A H13C 109.5 . .
H13A C13A H13C 109.5 . .
H13B C13A H13C 109.5 . .
N24A C14A H14A 109.5 . .
N24A C14A H14B 109.5 . .
H14A C14A H14B 109.5 . .
N24A C14A H14C 109.5 . .
H14A C14A H14C 109.5 . .
H14B C14A H14C 109.5 . .
N21A C22A C23A 109.7(2) . .
N21A C22A H22A 109.7 . .
C23A C22A H22A 109.7 . .
N21A C22A H22B 109.7 . .
C23A C22A H22B 109.7 . .
H22A C22A H22B 108.2 . .
N24A C23A C22A 110.8(3) . .
N24A C23A H23A 109.5 . .
C22A C23A H23A 109.5 . .
N24A C23A H23B 109.5 . .
C22A C23A H23B 109.5 . .
H23A C23A H23B 108.1 . .
N24A C25A C26A 111.4(2) . .
N24A C25A H25A 109.3 . .
C26A C25A H25A 109.3 . .
N24A C25A H25B 109.3 . .
C26A C25A H25B 109.3 . .
H25A C25A H25B 108.0 . .
N21A C26A C25A 108.2(3) . .
N21A C26A H26A 110.1 . .
C25A C26A H26A 110.1 . .
N21A C26A H26B 110.1 . .
C25A C26A H26B 110.1 . .
H26A C26A H26B 108.4 . .
C4B O1B Mg 124.66(19) . .
C1B O11B Mg 130.17(17) . .
C8B O2B C11B 112.3(2) . .
C2B N1B C9B 120.0(3) . .
C2B N1B C12B 119.4(3) . .
C9B N1B C12B 120.6(2) . .
C7B N21B C26B 116.9(2) . .
C7B N21B C22B 119.0(2) . .
C26B N21B C22B 112.0(2) . .
C23B N24B C25B 109.4(2) . .
C23B N24B C14B 110.5(3) . .
C25B N24B C14B 111.1(3) . .
O12B C1B O11B 122.9(2) . .
O12B C1B C3B 117.8(3) . .
O11B C1B C3B 119.3(3) . .
N1B C2B C3B 123.9(3) . .
N1B C2B H2B 118.0 . .
C3B C2B H2B 118.0 . .
C2B C3B C4B 119.5(2) . .
C2B C3B C1B 116.1(3) . .
C4B C3B C1B 124.4(3) . .
O1B C4B C3B 125.2(2) . .
O1B C4B C10B 119.0(3) . .
C3B C4B C10B 115.8(3) . .
C6B C5B C10B 118.6(3) . .
C6B C5B H5B 120.7 . .
C10B C5B H5B 120.7 . .
C5B C6B F1B 116.5(3) . .
C5B C6B C7B 125.2(3) . .
F1B C6B C7B 118.2(2) . .
C8B C7B C6B 115.9(3) . .
C8B C7B N21B 119.3(3) . .
C6B C7B N21B 124.8(3) . .
O2B C8B C7B 119.3(3) . .
O2B C8B C9B 120.1(3) . .
C7B C8B C9B 120.6(3) . .
N1B C9B C10B 119.6(2) . .
N1B C9B C8B 119.9(3) . .
C10B C9B C8B 120.4(3) . .
C5B C10B C9B 119.2(3) . .
C5B C10B C4B 119.9(3) . .
C9B C10B C4B 120.9(3) . .
O2B C11B C12B 112.8(3) . .
O2B C11B H11C 109.0 . .
C12B C11B H11C 109.0 . .
O2B C11B H11D 109.0 . .
C12B C11B H11D 109.0 . .
H11C C11B H11D 107.8 . .
N1B C12B C11B 107.9(3) . .
N1B C12B C13B 109.2(3) . .
C11B C12B C13B 112.5(3) . .
N1B C12B H12B 109.1 . .
C11B C12B H12B 109.1 . .
C13B C12B H12B 109.1 . .
C12B C13B H13D 109.5 . .
C12B C13B H13E 109.5 . .
H13D C13B H13E 109.5 . .
C12B C13B H13F 109.5 . .
H13D C13B H13F 109.5 . .
H13E C13B H13F 109.5 . .
N24B C14B H14D 109.5 . .
N24B C14B H14E 109.5 . .
H14D C14B H14E 109.5 . .
N24B C14B H14F 109.5 . .
H14D C14B H14F 109.5 . .
H14E C14B H14F 109.5 . .
N21B C22B C23B 109.2(3) . .
N21B C22B H22C 109.8 . .
```

```
C23B C22B H22C 109.8 . .
N21B C22B H22D 109.8 . .
C23B C22B H22D 109.8 . .
H22C C22B H22D 108.3 . .
N24B C23B C22B 110.7(3) . .
N24B C23B H23C 109.5 . .
C22B C23B H23C 109.5 . .
N24B C23B H23D 109.5 . .
C22B C23B H23D 109.5 . .
H23C C23B H23D 108.1 . .
N24B C25B C26B 110.6(3) . .
N24B C25B H25C 109.5 . .
C26B C25B H25C 109.5 . .
N24B C25B H25D 109.5 . .
C26B C25B H25D 109.5 . .
H25C C25B H25D 108.1 . .
N21B C26B C25B 110.6(2) . .
N21B C26B H26C 109.5 . .
C25B C26B H26C 109.5 . .
N21B C26B H26D 109.5 . .
C25B C26B H26D 109.5 . .
H26C C26B H26D 108.1 . .
Mg O1M H11M 123.5(16) . .
Mg O1M H12M 118(3) . .
H11M O1M H12M 103(3) . .
Mg O2M H21M 121(2) . .
Mg O2M H22M 138(5) . .
H21M O2M H22M 91(6) . .
H1W O1W H2W 108(4) . .
H3W O2W H4W 102(3) . .

loop_
 _geom_torsion_atom_site_label_1
 _geom_torsion_atom_site_label_2
 _geom_torsion_atom_site_label_3
 _geom_torsion_atom_site_label_4
 _geom_torsion
 _geom_torsion_site_symmetry_1
 _geom_torsion_site_symmetry_2
 _geom_torsion_site_symmetry_3
 _geom_torsion_site_symmetry_4
 _geom_torsion_publ_flag
O11A Mg O1A C4A 29.7(2) . . . .
O11B Mg O1A C4A -151.3(2) . . . .
O1B Mg O1A C4A 9(15) . . . .
O2M Mg O1A C4A -60.2(2) . . . .
O1M Mg O1A C4A 119.5(2) . . . .
O11B Mg O11A C1A -142(5) . . . .
O1B Mg O11A C1A 164.0(3) . . . .
O1A Mg O11A C1A -15.9(3) . . . .
O2M Mg O11A C1A 73.5(3) . . . .
O1M Mg O11A C1A -106.1(3) . . . .
Mg O11A C1A O12A 178.4(2) . . . .
Mg O11A C1A C3A -2.6(4) . . . .
C9A N1A C2A C3A 2.5(5) . . . .
C12A N1A C2A C3A 179.9(4) . . . .
N1A C2A C3A C4A 1.5(5) . . . .
N1A C2A C3A C1A -178.5(3) . . . .
O12A C1A C3A C2A 16.6(4) . . . .
O11A C1A C3A C2A -162.5(3) . . . .
O12A C1A C3A C4A -163.3(3) . . . .
O11A C1A C3A C4A 17.6(5) . . . .
Mg O1A C4A C3A -26.1(4) . . . .
Mg O1A C4A C10A 155.79(19) . . . .
C2A C3A C4A O1A 178.1(3) . . . .
C1A C3A C4A O1A -2.0(5) . . . .
C2A C3A C4A C10A -3.8(4) . . . .
C1A C3A C4A C10A 176.1(3) . . . .
C10A C5A C6A F1A -176.1(3) . . . .
C10A C5A C6A C7A 2.7(4) . . . .
C26A N21A C7A C8A -29.4(5) . . . .
C22A N21A C7A C8A 111.4(3) . . . .
C26A N21A C7A C6A 147.6(3) . . . .
C22A N21A C7A C6A -71.6(4) . . . .
F1A C6A C7A C8A -179.4(3) . . . .
C5A C6A C7A C8A 1.8(5) . . . .
F1A C6A C7A N21A 3.4(4) . . . .
C5A C6A C7A N21A -175.4(3) . . . .
C11A O2A C8A C7A -155.6(3) . . . .
C11A O2A C8A C9A 27.3(4) . . . .
N21A C7A C8A O2A -5.9(5) . . . .
C6A C7A C8A O2A 177.0(3) . . . .
N21A C7A C8A C9A 171.1(3) . . . .
C6A C7A C8A C9A -5.9(4) . . . .
C2A N1A C9A C10A -3.8(4) . . . .
C12A N1A C9A C10A 178.8(3) . . . .
C2A N1A C9A C8A 176.5(3) . . . .
C12A N1A C9A C8A -0.9(5) . . . .
O2A C8A C9A N1A 2.4(4) . . . .
C7A C8A C9A N1A -174.6(3) . . . .
O2A C8A C9A C10A -177.3(3) . . . .
C7A C8A C9A C10A 5.7(4) . . . .
N1A C9A C10A C5A 179.3(3) . . . .
C8A C9A C10A C5A -1.0(4) . . . .
N1A C9A C10A C4A 1.2(4) . . . .
C8A C9A C10A C4A -179.1(3) . . . .
C6A C5A C10A C9A -3.1(4) . . . .
C6A C5A C10A C4A 175.0(3) . . . .
O1A C4A C10A C9A -179.2(3) . . . .
C3A C4A C10A C9A 2.5(4) . . . .
O1A C4A C10A C5A 2.7(4) . . . .
C3A C4A C10A C5A -175.6(3) . . . .
C2A N1A C12A C13A -77.0(5) . . . .
C9A N1A C12A C13A 100.4(4) . . . .
C2A N1A C12A C11A 154.2(3) . . . .
C9A N1A C12A C11A -28.5(5) . . . .
C8A O2A C11A C12A -58.5(4) . . . .
C13A C12A C11A O2A -69.0(5) . . . .
N1A C12A C11A O2A 57.6(4) . . . .
C7A N21A C22A C23A 157.9(3) . . . .
C26A N21A C22A C23A -57.9(3) . . . .
C25A N24A C23A C22A -57.8(3) . . . .
C14A N24A C23A C22A -178.9(3) . . . .
N21A C22A C23A N24A 57.1(3) . . . .
C23A N24A C25A C26A 58.9(4) . . . .
C14A N24A C25A C26A -179.7(3) . . . .
C7A N21A C26A C25A -159.8(3) . . . .
C22A N21A C26A C25A 57.7(3) . . . .
N24A C25A C26A N21A -58.1(4) . . . .
O11A Mg O1B C4B 148.7(2) . . . .
O11B Mg O1B C4B -30.3(2) . . . .
O1A Mg O1B C4B 170(100) . . . .
O2M Mg O1B C4B -121.3(2) . . . .
O1M Mg O1B C4B 59.0(2) . . . .
O11A Mg O11B C1B -36(6) . . . .
O1B Mg O11B C1B 18.0(3) . . . .
O1A Mg O11B C1B -162.1(2) . . . .
O2M Mg O11B C1B 108.4(3) . . . .
```

```
O1M Mg O11B C1B -71.9(3) . . . .
Mg O11B C1B O12B 179.1(2) . . . .
Mg O11B C1B C3B 0.6(4) . . . .
C9B N1B C2B C3B -2.4(5) . . . .
C12B N1B C2B C3B 179.1(3) . . . .
N1B C2B C3B C4B -1.0(4) . . . .
N1B C2B C3B C1B 177.5(3) . . . .
O12B C1B C3B C2B -15.3(4) . . . .
O11B C1B C3B C2B 163.3(3) . . . .
O12B C1B C3B C4B 163.1(3) . . . .
O11B C1B C3B C4B -18.3(4) . . . .
Mg O1B C4B C3B 24.5(4) . . . .
Mg O1B C4B C10B -156.5(2) . . . .
C2B C3B C4B O1B -176.8(3) . . . .
C1B C3B C4B O1B 4.9(5) . . . .
C2B C3B C4B C10B 4.1(4) . . . .
C1B C3B C4B C10B -174.2(3) . . . .
C10B C5B C6B F1B -178.7(3) . . . .
C10B C5B C6B C7B 0.7(5) . . . .
C5B C6B C7B C8B -3.9(5) . . . .
F1B C6B C7B C8B 175.6(3) . . . .
C5B C6B C7B N21B 174.2(3) . . . .
F1B C6B C7B N21B -6.3(5) . . . .
C26B N21B C7B C8B -70.4(4) . . . .
C22B N21B C7B C8B 150.0(3) . . . .
C26B N21B C7B C6B 111.5(4) . . . .
C22B N21B C7B C6B -28.0(4) . . . .
C11B O2B C8B C7B 153.3(3) . . . .
C11B O2B C8B C9B -30.4(4) . . . .
C6B C7B C8B O2B -179.8(3) . . . .
N21B C7B C8B O2B 2.0(4) . . . .
C6B C7B C8B C9B 4.0(4) . . . .
N21B C7B C8B C9B -174.3(3) . . . .
C2B N1B C9B C10B 2.2(4) . . . .
C12B N1B C9B C10B -179.3(3) . . . .
C2B N1B C9B C8B -175.1(3) . . . .
C12B N1B C9B C8B 3.4(4) . . . .
O2B C8B C9B N1B -0.1(4) . . . .
C7B C8B C9B N1B 176.1(3) . . . .
O2B C8B C9B C10B -177.4(3) . . . .
C7B C8B C9B C10B -1.2(4) . . . .
C6B C5B C10B C9B 2.3(4) . . . .
C6B C5B C10B C4B -178.2(3) . . . .
N1B C9B C10B C5B -179.4(3) . . . .
C8B C9B C10B C5B -2.1(4) . . . .
N1B C9B C10B C4B 1.2(4) . . . .
C8B C9B C10B C4B 178.5(3) . . . .
O1B C4B C10B C5B -2.8(4) . . . .
C3B C4B C10B C5B 176.3(2) . . . .
O1B C4B C10B C9B 176.6(3) . . . .
C3B C4B C10B C9B -4.3(4) . . . .
C8B O2B C11B C12B 58.7(4) . . . .
C2B N1B C12B C11B -159.1(3) . . . .
C9B N1B C12B C11B 22.4(4) . . . .
C2B N1B C12B C13B 78.4(3) . . . .
C9B N1B C12B C13B -100.1(3) . . . .
O2B C11B C12B N1B -52.9(4) . . . .
O2B C11B C12B C13B 67.6(4) . . . .
C7B N21B C22B C23B -163.1(3) . . . .
C26B N21B C22B C23B 55.5(4) . . . .
C25B N24B C23B C22B 61.0(4) . . . .
C14B N24B C23B C22B -176.4(3) . . . .
N21B C22B C23B N24B -58.5(4) . . . .
C23B N24B C25B C26B -59.4(3) . . . .
C14B N24B C25B C26B 178.4(3) . . . .
C7B N21B C26B C25B 162.9(3) . . . .
C22B N21B C26B C25B -54.8(4) . . . .
N24B C25B C26B N21B 56.4(4) . . . .

loop_
 _geom_hbond_atom_site_label_D
 _geom_hbond_atom_site_label_H
 _geom_hbond_atom_site_label_A
 _geom_hbond_distance_DH
 _geom_hbond_distance_HA
 _geom_hbond_distance_DA
 _geom_hbond_angle_DHA
 _geom_hbond_site_symmetry_A
O1M H11M O12A  0.89(3) 1.83(3)
2.710(3) 171(2) 2_454
O1M H12M O2W  0.79(4) 1.96(4)
2.719(3) 160(4) 2_454
O2M H21M O1W  1.05(5) 1.68(5)
2.705(3) 163(4) .
O2M H22M O12B  0.93(8) 1.83(8)
2.712(3) 158(7) 2_544
O1W H1W O12B  0.75(5) 2.02(5)
2.755(3) 165(4) 1_545
O1W H2W O11B  1.10(5) 1.80(5)
2.894(3) 170(5) 2_544
O2W H3W O12A  0.99(4) 1.80(4)
2.760(3) 164(3) 2_454
O2W H4W O11A  0.88(4) 2.00(4)
2.869(3) 168(3) .
```

```
#  CIF produced by WinGX routine CIF_UPDATE
#  Created on 2005-02-17 at 09:47:16
#  Using CIFtbx version 2.6.2 16 Jun 1998

#     CCDC ELECTRONIC DATA DEPOSITION FORM (CIF)

data_global

_publ_contact_author               'Turel, Iztok'
_publ_contact_author_email          iztok.turel@uni-lj.si
_publ_contact_author_address
;
  Faculty of Chemistry and Chemical Technology
  University of Ljubljana
  Askerceva 5
  SI-1001 Ljubljana
  SLOVENIA
;
_publ_contact_author_phone              '+386 1 2419 124'
_publ_contact_author_fax                '+386 1 2419 220'

loop_
_publ_author_name
;
Dreven\<sek, Petra
Ko\<smrlj, Janez
Turel, Iztok
Giester, Gerald
Skauge, Tormod
Sletten, Einar
Sep\<ci\<c, Kristina
;

_journal_name_full
;
Journal of Inorganic Biochemistry
;
_journal_volume
_journal_page_first
_journal_page_last
_journal_year
_ccdc_journal_depnumber

data_cpd2

_audit_creation_date            2005-02-17T09:47:16-00:00
_audit_creation_method         'WinGX routine CIF_UPDATE'

#------------------------------------------------------------------------------#
#                   CHEMICAL INFORMATION                                       #
#------------------------------------------------------------------------------#

_chemical_formula_sum                   'C36 H46 F2 Mg N6 O12'
_chemical_formula_weight                817.1
_chemical_compound_source               'synthesis as described'
_chemical_absolute_configuration        syn

#------------------------------------------------------------------------------#
#                   UNIT CELL INFORMATION                                      #
#------------------------------------------------------------------------------#

_symmetry_cell_setting                  monoclinic
_symmetry_space_group_name_H-M          P21
```

```
loop_
    _symmetry_equiv_pos_as_xyz
'x, y, z'
'-x, y+1/2, -z'

_cell_length_a                          10.9761(4)
_cell_length_b                          9.7345(4)
_cell_length_c                          17.9179(8)
_cell_angle_alpha                       90.000(2)
_cell_angle_beta                        98.219(2)
_cell_angle_gamma                       90.000(2)
_cell_volume                            1894.81(13)
_cell_formula_units_Z                   2
_cell_measurement_temperature           150(2)

#-------------------------------------------------------------------------------#
#                   CRYSTAL INFORMATION                                         #
#-------------------------------------------------------------------------------#

_exptl_crystal_description              prism
_exptl_crystal_colour                   yellow
_exptl_crystal_size_max                 0.15
_exptl_crystal_size_mid                 0.1
_exptl_crystal_size_min                 0.05
_exptl_crystal_density_diffrn           1.432
_exptl_crystal_density_method           'not measured'
_exptl_crystal_F_000                    860
_exptl_special_details
;
238 frames in 6 sets of \w scans. Rotation/frame 1.8\%.
Crystal-detector distance=35 mm. Measuring time=43 s/\%.
;

#-------------------------------------------------------------------------------#
#                   ABSORPTION CORRECTION                                       #
#-------------------------------------------------------------------------------#

_exptl_absorpt_coefficient_mu           0.129
_exptl_absorpt_correction_type          'multi-scan (Otwinovski & Minor, 1997)'
_exptl_absorpt_correction_T_min         0.985
_exptl_absorpt_correction_T_max         0.994

#-------------------------------------------------------------------------------#
#                   DATA COLLECTION                                             #
#-------------------------------------------------------------------------------#

_diffrn_ambient_temperature             150(2)
_diffrn_radiation_wavelength            0.71073
_diffrn_radiation_probe                 x-rey
_diffrn_radiation_type                  MoK\a
_diffrn_radiation_monochromator         graphite
_diffrn_radiation_source                'fine-focus sealed tube'
_diffrn_measurement_device              'Nonius KappaCCD diffractometer'
_diffrn_measurement_method              '\w scans'
_diffrn_reflns_av_R_equivalents         0.069
_diffrn_reflns_av_unetI/netI            0.0807
_diffrn_reflns_number                   14536
_diffrn_reflns_limit_h_min              -13
_diffrn_reflns_limit_h_max              13
_diffrn_reflns_limit_k_min              -12
_diffrn_reflns_limit_k_max              12
_diffrn_reflns_limit_l_min              -22
_diffrn_reflns_limit_l_max              22
_diffrn_reflns_theta_min                3.45
```

```
_diffrn_reflns_theta_max                26.37
_diffrn_reflns_theta_full               26.37
_diffrn_measured_fraction_theta_full    0.997
_diffrn_measured_fraction_theta_max     0.997
_reflns_number_total                    7654
_reflns_number_gt                       5372
_reflns_threshold_expression            >2sigma(I)

#---------------------------------------------------------------------------#
#                   COMPUTER PROGRAMS USED                                  #
#---------------------------------------------------------------------------#

_computing_data_collection              'COLLECT (Nonius, 1999)'
_computing_cell_refinement
;
DENZO and SCALEPACK (Otwinovski & Minor, 1997)
;
_computing_data_reduction
;
DENZO and SCALEPACK (Otwinovski & Minor, 1997)'
;
_computing_structure_solution           'SHELXS-97 (Sheldrick, 1997)'
_computing_structure_refinement         'SHELXL-97 (Sheldrick, 1997)'
_computing_molecular_graphics
;
PLUTON (Spek, 1991),
PLATON (Spek, 2003),
ORTEP-3 (Farrugia, 1999),
MERCURY (Bruno et al., 2002)
;
_computing_publication_material
;
WinGX publication routines (Farrugia, 1999)
;

#---------------------------------------------------------------------------#
#                   REFINEMENT INFORMATION                                  #
#---------------------------------------------------------------------------#

_refine_special_details
;
 Refinement of F^2^ against ALL reflections.  The weighted R-factor wR and
 goodness of fit S are based on F^2^, conventional R-factors R are based
 on F, with F set to zero for negative F^2^. The threshold expression of
 F^2^ > 2sigma(F^2^) is used only for calculating R-factors(gt) etc. and is
 not relevant to the choice of reflections for refinement.  R-factors based
 on F^2^ are statistically about twice as large as those based on F, and R-
 factors based on ALL data will be even larger.
;
_refine_ls_structure_factor_coef        Fsqd
_refine_ls_matrix_type                  full
_refine_ls_weighting_scheme             calc
_refine_ls_weighting_details
         'calc w=1/[\s^2^(Fo^2^)+(0.0485P)^2^+0.0285P] where P=(Fo^2^+2Fc^2^)/3'
_atom_sites_solution_primary            direct
_atom_sites_solution_secondary          difmap
_atom_sites_solution_hydrogens          difmap
_refine_ls_hydrogen_treatment           refall
_refine_ls_extinction_method            SHELXL97
_refine_ls_extinction_expression
                                    Fc^*^=kFc[1+0.001xFc^2^\l^3^/sin(2\q)]^-1/4^
_refine_ls_extinction_coef              0.0034(7)
_refine_ls_number_reflns                7654
_refine_ls_number_parameters            547
```

```
_refine_ls_number_restraints            1
_refine_ls_R_factor_all                 0.0914
_refine_ls_R_factor_gt                  0.0489
_refine_ls_wR_factor_ref                0.1078
_refine_ls_wR_factor_gt                 0.0927
_refine_ls_goodness_of_fit_ref          1.011
_refine_ls_restrained_S_all             1.011
_refine_ls_shift/su_max                 0.001
_refine_ls_shift/su_mean                0.000
_refine_ls_abs_structure_details        'Flack (1983), Acta Cryst. A39, 876-881'
_refine_ls_abs_structure_Flack          0.1(3)
_refine_diff_density_max                0.266
_refine_diff_density_min                -0.237
_refine_diff_density_rms                0.053

#-------------------------------------------------------------------------------#
#                    ATOMIC TYPES, COORDINATES AND THERMAL PARAMETERS           #
#-------------------------------------------------------------------------------#

loop_
    _atom_type_symbol
    _atom_type_description
    _atom_type_scat_dispersion_real
    _atom_type_scat_dispersion_imag
    _atom_type_scat_source
C C 0.0033 0.0016 'International Tables Vol C Tables 4.2.6.8 and 6.1.1.4'
H H 0 0 'International Tables Vol C Tables 4.2.6.8 and 6.1.1.4'
F F 0.0171 0.0103 'International Tables Vol C Tables 4.2.6.8 and 6.1.1.4'
Mg Mg 0.0486 0.0363 'International Tables Vol C Tables 4.2.6.8 and 6.1.1.4'
N N 0.0061 0.0033 'International Tables Vol C Tables 4.2.6.8 and 6.1.1.4'
O O 0.0106 0.006 'International Tables Vol C Tables 4.2.6.8 and 6.1.1.4'

loop_
 _atom_site_label
 _atom_site_type_symbol
 _atom_site_fract_x
 _atom_site_fract_y
 _atom_site_fract_z
 _atom_site_U_iso_or_equiv
 _atom_site_adp_type
 _atom_site_occupancy
 _atom_site_symmetry_multiplicity
 _atom_site_calc_flag
 _atom_site_refinement_flags
 _atom_site_disorder_assembly
 _atom_site_disorder_group
Mg1 Mg 0.24220(10) 0.68098(14) 0.49580(6) 0.0194(2) Uani 1 1 d . . .
O1M O 0.4078(2) 0.5914(3) 0.54465(13) 0.0247(5) Uani 1 1 d . . .
O2M O 0.0789(2) 0.7699(3) 0.44537(13) 0.0235(5) Uani 1 1 d . . .
F1A F 0.53765(16) 0.6760(2) 0.18825(10) 0.0328(5) Uani 1 1 d . . .
O1A O 0.28487(18) 0.6242(2) 0.39346(11) 0.0220(5) Uani 1 1 d . . .
O11A O 0.15906(18) 0.4960(2) 0.50094(11) 0.0225(5) Uani 1 1 d . . .
O12A O 0.12811(19) 0.2714(2) 0.48397(12) 0.0276(6) Uani 1 1 d . . .
O2A O 0.48549(19) 0.1926(2) 0.20549(11) 0.0280(6) Uani 1 1 d . . .
N1A N 0.3588(2) 0.2330(3) 0.32798(13) 0.0217(6) Uani 1 1 d . . .
N21A N 0.5610(2) 0.4093(3) 0.12481(14) 0.0255(7) Uani 1 1 d . . .
N24A N 0.6987(2) 0.3910(3) 0.00203(14) 0.0317(7) Uani 1 1 d . . .
C1A C 0.1756(3) 0.3835(4) 0.46774(17) 0.0200(7) Uani 1 1 d . . .
C2A C 0.2900(3) 0.2553(3) 0.38339(16) 0.0196(7) Uani 1 1 d . . .
H2A H 0.2614 0.1769 0.4073 0.024 Uiso 1 1 calc R . .
C3A C 0.2579(3) 0.3813(3) 0.40810(17) 0.0195(7) Uani 1 1 d . . .
C4A C 0.3033(3) 0.5022(3) 0.37486(17) 0.0198(8) Uani 1 1 d . . .
C5A C 0.4238(3) 0.5897(4) 0.27765(17) 0.0219(8) Uani 1 1 d . . .
H5A H 0.4106 0.6810 0.2934 0.026 Uiso 1 1 calc R . .
```

```
C6A C 0.4877(3) 0.5652(3) 0.21960(17) 0.0231(8) Uani 1 1 d . . .
C7A C 0.5086(3) 0.4344(3) 0.19017(18) 0.0222(8) Uani 1 1 d . . .
C8A C 0.4682(3) 0.3238(3) 0.22979(17) 0.0223(8) Uani 1 1 d . . .
C9A C 0.4034(3) 0.3451(4) 0.29148(16) 0.0205(7) Uani 1 1 d . . .
C10A C 0.3777(3) 0.4772(3) 0.31393(16) 0.0185(7) Uani 1 1 d . . .
C11A C 0.5000(3) 0.0952(4) 0.26727(17) 0.0299(8) Uani 1 1 d . . .
H11A H 0.5720 0.1214 0.3043 0.036 Uiso 1 1 calc R . .
H11B H 0.5156 0.0026 0.2478 0.036 Uiso 1 1 calc R . .
C12A C 0.3855(3) 0.0913(3) 0.30603(17) 0.0244(7) Uani 1 1 d . . .
H12A H 0.4048 0.0355 0.3531 0.029 Uiso 1 1 calc R . .
C13A C 0.2744(3) 0.0275(4) 0.25829(18) 0.0349(8) Uani 1 1 d . . .
H13A H 0.2042 0.0282 0.2865 0.052 Uiso 1 1 calc R . .
H13B H 0.2934 -0.0674 0.2458 0.052 Uiso 1 1 calc R . .
H13C H 0.2537 0.0805 0.2117 0.052 Uiso 1 1 calc R . .
C14A C 0.7255(3) 0.3361(4) -0.07000(18) 0.0432(9) Uani 1 1 d . . .
H14A H 0.8088 0.2975 -0.0633 0.065 Uiso 1 1 calc R . .
H14B H 0.7198 0.4102 -0.1074 0.065 Uiso 1 1 calc R . .
H14C H 0.6659 0.2641 -0.0875 0.065 Uiso 1 1 calc R . .
C22A C 0.5498(3) 0.5150(4) 0.06578(17) 0.0399(9) Uani 1 1 d . . .
H22A H 0.6090 0.5903 0.0806 0.048 Uiso 1 1 calc R . .
H22B H 0.4657 0.5541 0.0589 0.048 Uiso 1 1 calc R . .
C23A C 0.5761(3) 0.4504(4) -0.00733(19) 0.0396(10) Uani 1 1 d . . .
H23A H 0.5144 0.3779 -0.0230 0.047 Uiso 1 1 calc R . .
H23B H 0.5692 0.5210 -0.0474 0.047 Uiso 1 1 calc R . .
C25A C 0.7067(3) 0.2843(4) 0.05892(17) 0.0326(8) Uani 1 1 d . . .
H25A H 0.7900 0.2432 0.0653 0.039 Uiso 1 1 calc R . .
H25B H 0.6464 0.2110 0.0423 0.039 Uiso 1 1 calc R . .
C26A C 0.6811(3) 0.3421(4) 0.13355(16) 0.0301(8) Uani 1 1 d . . .
H26A H 0.6828 0.2669 0.1709 0.036 Uiso 1 1 calc R . .
H26B H 0.7459 0.4092 0.1526 0.036 Uiso 1 1 calc R . .
F1B F -0.02670(15) 0.67054(19) 0.81615(9) 0.0296(5) Uani 1 1 d . . .
O1B O 0.20291(18) 0.7318(2) 0.59954(11) 0.0224(5) Uani 1 1 d . . .
O11B O 0.32920(18) 0.8657(2) 0.49438(11) 0.0225(5) Uani 1 1 d . . .
O12B O 0.39211(19) 1.0760(2) 0.52832(12) 0.0259(5) Uani 1 1 d . . .
O2B O 0.01373(19) 1.1527(2) 0.80009(11) 0.0259(6) Uani 1 1 d . . .
N1B N 0.1695(2) 1.1148(3) 0.68888(13) 0.0198(6) Uani 1 1 d . . .
N21B N -0.0573(2) 0.9182(3) 0.87904(14) 0.0222(6) Uani 1 1 d . . .
N24B N -0.1852(2) 0.9517(3) 1.00508(14) 0.0275(7) Uani 1 1 d . . .
C1B C 0.3292(3) 0.9714(4) 0.53610(17) 0.0200(8) Uani 1 1 d . . .
C2B C 0.2358(3) 1.0964(3) 0.63267(16) 0.0196(7) Uani 1 1 d . . .
H2B H 0.2755 1.1742 0.6151 0.023 Uiso 1 1 calc R . .
C3B C 0.2503(3) 0.9714(3) 0.59844(17) 0.0181(7) Uani 1 1 d . . .
C4B C 0.1935(3) 0.8524(3) 0.62455(16) 0.0172(7) Uani 1 1 d . . .
C5B C 0.0707(3) 0.7602(3) 0.71907(16) 0.0210(7) Uani 1 1 d . . .
H5B H 0.0743 0.6709 0.6982 0.025 Uiso 1 1 calc R . .
C6B C 0.0139(3) 0.7822(4) 0.78098(16) 0.0198(8) Uani 1 1 d . . .
C7B C -0.0039(3) 0.9119(4) 0.81234(18) 0.0211(8) Uani 1 1 d . . .
C8B C 0.0391(3) 1.0241(3) 0.77557(17) 0.0198(7) Uani 1 1 d . . .
C9B C 0.1102(3) 1.0035(3) 0.71680(16) 0.0185(7) Uani 1 1 d . . .
C10B C 0.1235(3) 0.8726(3) 0.68724(17) 0.0194(7) Uani 1 1 d . . .
C11B C 0.0371(3) 1.2608(3) 0.74878(17) 0.0258(8) Uani 1 1 d . . .
H11C H 0.0267 1.3515 0.7721 0.031 Uiso 1 1 calc R . .
H11D H -0.0224 1.2544 0.7019 0.031 Uiso 1 1 calc R . .
C12B C 0.1669(3) 1.2471(3) 0.73055(16) 0.0222(7) Uani 1 1 d . . .
H12B H 0.2239 1.2388 0.7791 0.027 Uiso 1 1 calc R . .
C13B C 0.2074(3) 1.3697(3) 0.68766(17) 0.0279(7) Uani 1 1 d . . .
H13D H 0.2921 1.3554 0.6778 0.042 Uiso 1 1 calc R . .
H13E H 0.2036 1.4532 0.7178 0.042 Uiso 1 1 calc R . .
H13F H 0.1528 1.3795 0.6397 0.042 Uiso 1 1 calc R . .
C14B C -0.2156(3) 0.9097(4) 1.07834(18) 0.0401(9) Uani 1 1 d . . .
H14D H -0.1915 0.9823 1.1154 0.060 Uiso 1 1 calc R . .
H14E H -0.1714 0.8249 1.0945 0.060 Uiso 1 1 calc R . .
H14F H -0.3045 0.8936 1.0744 0.060 Uiso 1 1 calc R . .
C22B C -0.0187(3) 1.0238(4) 0.93539(16) 0.0307(8) Uani 1 1 d . . .
```

```
H22C H -0.0600 1.1119 0.9201 0.037 Uiso 1 1 calc R . .
H22D H 0.0714 1.0380 0.9399 0.037 Uiso 1 1 calc R . .
C23B C -0.0533(3) 0.9769(4) 1.01039(17) 0.0327(8) Uani 1 1 d . . .
H23C H -0.0079 0.8917 1.0265 0.039 Uiso 1 1 calc R . .
H23D H -0.0288 1.0482 1.0490 0.039 Uiso 1 1 calc R . .
C25B C -0.2210(3) 0.8449(4) 0.94867(16) 0.0309(8) Uani 1 1 d . . .
H25C H -0.3106 0.8279 0.9447 0.037 Uiso 1 1 calc R . .
H25D H -0.1776 0.7583 0.9646 0.037 Uiso 1 1 calc R . .
C26B C -0.1895(3) 0.8881(3) 0.87247(16) 0.0251(7) Uani 1 1 d . . .
H26C H -0.2110 0.8135 0.8354 0.030 Uiso 1 1 calc R . .
H26D H -0.2375 0.9707 0.8545 0.030 Uiso 1 1 calc R . .
O2W O 0.0399(2) 0.0363(3) 0.41348(14) 0.0284(6) Uani 1 1 d . . .
O1W O 0.5280(2) 0.8279(2) 0.41060(13) 0.0272(6) Uani 1 1 d . . .
H11M H 0.407(4) 0.510(5) 0.558(2) 0.063(16) Uiso 1 1 d . . .
H12M H 0.481(4) 0.588(4) 0.5236(19) 0.051(12) Uiso 1 1 d . . .
H21M H 0.018(3) 0.765(4) 0.4663(18) 0.036(11) Uiso 1 1 d . . .
H22M H 0.089(3) 0.867(5) 0.435(2) 0.058(13) Uiso 1 1 d . . .
H3W H -0.020(4) 0.030(5) 0.434(2) 0.062(15) Uiso 1 1 d . . .
H4W H 0.081(5) 0.124(6) 0.426(3) 0.12(2) Uiso 1 1 d . . .
H1W H 0.567(3) 0.742(4) 0.4336(17) 0.028(9) Uiso 1 1 d . . .
H2W H 0.466(3) 0.838(4) 0.4378(19) 0.047(12) Uiso 1 1 d . . .

loop_
 _atom_site_aniso_label
 _atom_site_aniso_U_11
 _atom_site_aniso_U_22
 _atom_site_aniso_U_33
 _atom_site_aniso_U_23
 _atom_site_aniso_U_13
 _atom_site_aniso_U_12
Mg1 0.0215(4) 0.0173(5) 0.0204(5) -0.0018(4) 0.0068(4) 0.0000(4)
O1M 0.0218(12) 0.0236(16) 0.0297(13) 0.0048(12) 0.0073(10) 0.0011(11)
O2M 0.0209(12) 0.0235(15) 0.0278(13) 0.0037(11) 0.0085(10) 0.0018(11)
F1A 0.0398(10) 0.0283(12) 0.0339(11) 0.0005(10) 0.0179(9) -0.0076(10)
O1A 0.0297(12) 0.0161(14) 0.0216(12) -0.0020(10) 0.0082(10) 0.0012(10)
O11A 0.0262(11) 0.0172(13) 0.0254(12) -0.0018(11) 0.0082(9) -0.0015(10)
O12A 0.0301(12) 0.0236(14) 0.0320(13) -0.0048(11) 0.0147(10) -0.0040(11)
O2A 0.0411(13) 0.0252(14) 0.0196(12) -0.0023(11) 0.0107(10) 0.0105(12)
N1A 0.0263(14) 0.0190(15) 0.0202(14) -0.0008(12) 0.0051(12) 0.0056(12)
N21A 0.0252(14) 0.0342(17) 0.0182(14) 0.0042(13) 0.0069(11) 0.0089(13)
N24A 0.0308(15) 0.0426(19) 0.0245(16) -0.0013(15) 0.0133(13) 0.0007(14)
C1A 0.0212(16) 0.014(2) 0.0250(18) -0.0024(16) 0.0036(14) -0.0046(15)
C2A 0.0207(15) 0.0212(19) 0.0174(16) 0.0030(14) 0.0041(13) -0.0011(14)
C3A 0.0210(15) 0.0190(19) 0.0179(17) -0.0039(15) 0.0010(13) -0.0001(15)
C4A 0.0195(15) 0.021(2) 0.0182(18) -0.0005(16) -0.0009(13) 0.0026(15)
C5A 0.0225(16) 0.022(2) 0.0216(17) -0.0050(16) 0.0036(14) -0.0020(15)
C6A 0.0226(17) 0.022(2) 0.0240(18) 0.0022(16) 0.0020(15) -0.0010(15)
C7A 0.0187(16) 0.031(2) 0.0169(18) 0.0036(16) 0.0032(14) 0.0021(15)
C8A 0.0232(16) 0.026(2) 0.0169(17) -0.0068(16) -0.0006(14) 0.0086(15)
C9A 0.0209(16) 0.021(2) 0.0188(17) 0.0024(15) 0.0006(13) 0.0023(15)
C10A 0.0172(15) 0.024(2) 0.0135(16) -0.0009(15) 0.0008(13) -0.0003(15)
C11A 0.0366(19) 0.025(2) 0.0289(19) 0.0025(16) 0.0082(15) 0.0085(16)
C12A 0.0312(18) 0.0188(17) 0.0232(17) -0.0018(14) 0.0037(14) 0.0110(14)
C13A 0.0359(19) 0.028(2) 0.040(2) -0.0082(17) 0.0006(16) 0.0087(16)
C14A 0.044(2) 0.057(3) 0.033(2) -0.0078(19) 0.0206(16) -0.0035(19)
C22A 0.048(2) 0.044(2) 0.0293(19) 0.0039(18) 0.0129(17) 0.0156(18)
C23A 0.041(2) 0.053(3) 0.0261(19) 0.0068(17) 0.0126(16) 0.0134(19)
C25A 0.0287(16) 0.040(2) 0.0307(19) -0.0065(16) 0.0094(14) 0.0029(16)
C26A 0.0249(16) 0.043(2) 0.0225(16) -0.0029(16) 0.0044(13) 0.0050(15)
F1B 0.0347(10) 0.0296(12) 0.0271(10) -0.0008(9) 0.0127(8) -0.0062(10)
O1B 0.0283(12) 0.0182(14) 0.0219(12) -0.0012(11) 0.0076(10) -0.0019(10)
O11B 0.0247(11) 0.0192(14) 0.0253(12) -0.0068(11) 0.0098(9) -0.0029(10)
O12B 0.0313(12) 0.0145(13) 0.0352(13) -0.0018(11) 0.0159(10) -0.0066(10)
O2B 0.0343(12) 0.0207(15) 0.0247(12) -0.0022(11) 0.0115(10) 0.0014(11)
```

```
N1B 0.0220(13) 0.0164(15) 0.0216(14) -0.0030(12) 0.0052(11) 0.0018(11)
N21B 0.0177(13) 0.0326(17) 0.0170(14) -0.0046(12) 0.0054(11) -0.0038(12)
N24B 0.0264(15) 0.0387(19) 0.0191(14) -0.0012(13) 0.0092(12) 0.0050(14)
C1B 0.0174(15) 0.022(2) 0.0202(18) 0.0013(16) 0.0029(14) 0.0071(15)
C2B 0.0228(16) 0.0195(18) 0.0171(16) -0.0025(14) 0.0051(14) 0.0006(14)
C3B 0.0125(14) 0.0202(19) 0.0219(18) 0.0004(15) 0.0036(13) 0.0000(14)
C4B 0.0156(15) 0.019(2) 0.0166(16) -0.0026(15) 0.0010(13) 0.0004(14)
C5B 0.0228(16) 0.019(2) 0.0197(17) -0.0025(15) -0.0003(14) 0.0002(15)
C6B 0.0186(15) 0.023(2) 0.0178(17) 0.0055(16) 0.0028(14) -0.0065(15)
C7B 0.0190(16) 0.027(2) 0.0174(18) -0.0057(15) 0.0016(14) -0.0006(15)
C8B 0.0187(15) 0.0193(19) 0.0212(18) -0.0020(16) 0.0018(14) 0.0031(15)
C9B 0.0183(15) 0.021(2) 0.0163(16) -0.0003(15) 0.0019(13) 0.0003(14)
C10B 0.0207(16) 0.018(2) 0.0188(16) -0.0014(15) 0.0008(13) -0.0001(14)
C11B 0.0312(17) 0.0212(19) 0.0262(18) -0.0009(15) 0.0083(14) 0.0068(15)
C12B 0.0272(16) 0.0187(17) 0.0208(16) -0.0034(14) 0.0036(13) 0.0040(14)
C13B 0.0358(18) 0.0178(17) 0.0307(18) -0.0047(15) 0.0071(14) 0.0008(14)
C14B 0.037(2) 0.059(3) 0.0252(19) 0.0038(18) 0.0102(15) 0.0049(18)
C22B 0.0243(16) 0.045(2) 0.0235(17) -0.0092(16) 0.0068(13) -0.0072(15)
C23B 0.0319(17) 0.046(2) 0.0203(17) -0.0087(16) 0.0039(14) -0.0018(16)
C25B 0.0259(16) 0.037(2) 0.0301(18) 0.0049(16) 0.0059(14) -0.0002(15)
C26B 0.0229(16) 0.0339(19) 0.0189(16) 0.0015(14) 0.0043(13) -0.0012(14)
O2W 0.0269(13) 0.0236(15) 0.0366(15) -0.0015(12) 0.0107(11) 0.0032(12)
O1W 0.0282(13) 0.0226(15) 0.0329(14) 0.0022(12) 0.0116(11) 0.0026(11)

#------------------------------------------------------------------------------#
#                    MOLECULAR GEOMETRY                                        #
#------------------------------------------------------------------------------#

_geom_special_details
;
 All esds (except the esd in the dihedral angle between two l.s. planes)
 are estimated using the full covariance matrix.  The cell esds are taken
 into account individually in the estimation of esds in distances, angles
 and torsion angles; correlations between esds in cell parameters are only
 used when they are defined by crystal symmetry.  An approximate (isotropic)
 treatment of cell esds is used for estimating esds involving l.s. planes.
;

loop_
 _geom_bond_atom_site_label_1
 _geom_bond_atom_site_label_2
 _geom_bond_distance
 _geom_bond_site_symmetry_2
 _geom_bond_publ_flag
Mg1 O11A 2.027(2) .
Mg1 O1B 2.029(2) .
Mg1 O1A 2.033(2) .
Mg1 O11B 2.038(3) .
Mg1 O2M 2.077(2) .
Mg1 O1M 2.092(2) .
O1M H11M 0.83(5) .
O1M H12M 0.93(4) .
O2M H21M 0.81(3) .
O2M H22M 0.97(5) .
F1A C6A 1.367(4) .
O1A C4A 1.258(4) .
O11A C1A 1.272(4) .
O12A C1A 1.261(4) .
O2A C8A 1.372(4) .
O2A C11A 1.449(4) .
N1A C2A 1.348(4) .
N1A C9A 1.397(4) .
N1A C12A 1.475(4) .
N21A C7A 1.398(4) .
N21A C26A 1.460(4) .
N21A C22A 1.468(4) .
N24A C25A 1.449(4) .
N24A C23A 1.451(4) .
N24A C14A 1.465(4) .
C1A C3A 1.495(4) .
C2A C3A 1.368(4) .
C2A H2A 0.9500 .
C3A C4A 1.440(5) .
C4A C10A 1.474(4) .
C5A C6A 1.356(4) .
C5A C10A 1.404(4) .
C5A H5A 0.9500 .
C6A C7A 1.409(4) .
C7A C8A 1.396(4) .
C8A C9A 1.413(4) .
C9A C10A 1.388(5) .
C11A C12A 1.521(4) .
C11A H11A 0.9900 .
C11A H11B 0.9900 .
C12A C13A 1.519(4) .
C12A H12A 1.0000 .
C13A H13A 0.9800 .
C13A H13B 0.9800 .
C13A H13C 0.9800 .
C14A H14A 0.9800 .
```

```
C14A H14B 0.9800 .
C14A H14C 0.9800 .
C22A C23A 1.518(4) .
C22A H22A 0.9900 .
C22A H22B 0.9900 .
C23A H23A 0.9900 .
C23A H23B 0.9900 .
C25A C26A 1.514(4) .
C25A H25A 0.9900 .
C25A H25B 0.9900 .
C26A H26A 0.9900 .
C26A H26B 0.9900 .
F1B C6B 1.363(4) .
O1B C4B 1.266(4) .
O11B C1B 1.272(4) .
O12B C1B 1.249(4) .
O2B C8B 1.368(4) .
O2B C11B 1.444(4) .
N1B C2B 1.336(4) .
N1B C9B 1.393(4) .
N1B C12B 1.491(4) .
N21B C7B 1.406(4) .
N21B C22B 1.461(4) .
N21B C26B 1.468(4) .
N24B C23B 1.458(4) .
N24B C14B 1.459(4) .
N24B C25B 1.464(4) .
C1B C3B 1.508(4) .
C2B C3B 1.382(4) .
C2B H2B 0.9500 .
C3B C4B 1.426(4) .
C4B C10B 1.462(4) .
C5B C6B 1.365(4) .
C5B C10B 1.397(4) .
C5B H5B 0.9500 .
C6B C7B 1.406(4) .
C7B C8B 1.393(5) .
C8B C9B 1.412(4) .
C9B C10B 1.396(5) .
C11B C12B 1.512(4) .
C11B H11C 0.9900 .
C11B H11D 0.9900 .
C12B C13B 1.520(4) .
C12B H12B 1.0000 .
C13B H13D 0.9800 .
C13B H13E 0.9800 .
C13B H13F 0.9800 .
C14B H14D 0.9800 .
C14B H14E 0.9800 .
C14B H14F 0.9800 .
C22B C23B 1.518(4) .
C22B H22C 0.9900 .
C22B H22D 0.9900 .
C23B H23C 0.9900 .
C23B H23D 0.9900 .
C25B C26B 1.515(4) .
C25B H25C 0.9900 .
C25B H25D 0.9900 .
C26B H26C 0.9900 .
C26B H26D 0.9900 .
O2W H3W 0.80(4) .
O2W H4W 0.97(6) .
O1W H1W 1.00(3) .
O1W H2W 0.90(4) .
```

```
loop_
 _geom_angle_atom_site_label_1
 _geom_angle_atom_site_label_2
 _geom_angle_atom_site_label_3
 _geom_angle
 _geom_angle_site_symmetry_1
 _geom_angle_site_symmetry_3
 _geom_angle_publ_flag
O11A Mg1 O1B 91.09(9) . .
O11A Mg1 O1A 87.87(10) . .
O1B Mg1 O1A 178.00(13) . .
O11A Mg1 O11B 177.94(11) . .
O1B Mg1 O11B 87.56(9) . .
O1A Mg1 O11B 93.42(9) . .
O11A Mg1 O2M 91.38(10) . .
O1B Mg1 O2M 90.78(10) . .
O1A Mg1 O2M 90.95(10) . .
O11B Mg1 O2M 90.20(11) . .
O11A Mg1 O1M 88.88(11) . .
O1B Mg1 O1M 90.24(10) . .
O1A Mg1 O1M 88.03(10) . .
O11B Mg1 O1M 89.56(10) . .
O2M Mg1 O1M 178.94(13) . .
Mg1 O1M H11M 118(3) . .
Mg1 O1M H12M 126(2) . .
H11M O1M H12M 98(4) . .
Mg1 O2M H21M 119(2) . .
Mg1 O2M H22M 112(2) . .
H21M O2M H22M 106(4) . .
C4A O1A Mg1 124.2(2) . .
C1A O11A Mg1 130.4(2) . .
C8A O2A C11A 111.9(2) . .
C2A N1A C9A 119.3(3) . .
C2A N1A C12A 120.0(3) . .
C9A N1A C12A 120.7(2) . .
C7A N21A C26A 117.5(2) . .
C7A N21A C22A 118.6(3) . .
C26A N21A C22A 111.9(2) . .
C25A N24A C23A 109.2(2) . .
C25A N24A C14A 111.0(3) . .
C23A N24A C14A 110.1(3) . .
O12A C1A O11A 123.1(3) . .
O12A C1A C3A 117.7(3) . .
O11A C1A C3A 119.2(3) . .
N1A C2A C3A 125.5(3) . .
N1A C2A H2A 117.3 . .
C3A C2A H2A 117.3 . .
C2A C3A C4A 118.6(3) . .
C2A C3A C1A 117.0(3) . .
C4A C3A C1A 124.4(3) . .
O1A C4A C3A 125.7(3) . .
O1A C4A C10A 118.7(3) . .
C3A C4A C10A 115.6(3) . .
C6A C5A C10A 118.6(3) . .
C6A C5A H5A 120.7 . .
C10A C5A H5A 120.7 . .
C5A C6A F1A 117.2(3) . .
C5A C6A C7A 125.1(3) . .
F1A C6A C7A 117.6(3) . .
C8A C7A N21A 119.3(3) . .
C8A C7A C6A 115.2(3) . .
N21A C7A C6A 125.4(3) . .
O2A C8A C7A 119.3(3) . .
```

```
O2A C8A C9A 119.5(3) . .
C7A C8A C9A 121.1(3) . .
C10A C9A N1A 119.3(3) . .
C10A C9A C8A 120.6(3) . .
N1A C9A C8A 120.1(3) . .
C9A C10A C5A 119.1(3) . .
C9A C10A C4A 121.7(3) . .
C5A C10A C4A 119.3(3) . .
O2A C11A C12A 110.9(2) . .
O2A C11A H11A 109.5 . .
C12A C11A H11A 109.5 . .
O2A C11A H11B 109.5 . .
C12A C11A H11B 109.5 . .
H11A C11A H11B 108.0 . .
N1A C12A C13A 111.0(2) . .
N1A C12A C11A 107.9(3) . .
C13A C12A C11A 113.7(2) . .
N1A C12A H12A 108.0 . .
C13A C12A H12A 108.0 . .
C11A C12A H12A 108.0 . .
C12A C13A H13A 109.5 . .
C12A C13A H13B 109.5 . .
H13A C13A H13B 109.5 . .
C12A C13A H13C 109.5 . .
H13A C13A H13C 109.5 . .
H13B C13A H13C 109.5 . .
N24A C14A H14A 109.5 . .
N24A C14A H14B 109.5 . .
H14A C14A H14B 109.5 . .
N24A C14A H14C 109.5 . .
H14A C14A H14C 109.5 . .
H14B C14A H14C 109.5 . .
N21A C22A C23A 108.9(3) . .
N21A C22A H22A 109.9 . .
C23A C22A H22A 109.9 . .
N21A C22A H22B 109.9 . .
C23A C22A H22B 109.9 . .
H22A C22A H22B 108.3 . .
N24A C23A C22A 110.7(3) . .
N24A C23A H23A 109.5 . .
C22A C23A H23A 109.5 . .
N24A C23A H23B 109.5 . .
C22A C23A H23B 109.5 . .
H23A C23A H23B 108.1 . .
N24A C25A C26A 110.8(3) . .
N24A C25A H25A 109.5 . .
C26A C25A H25A 109.5 . .
N24A C25A H25B 109.5 . .
C26A C25A H25B 109.5 . .
H25A C25A H25B 108.1 . .
N21A C26A C25A 110.5(2) . .
N21A C26A H26A 109.5 . .
C25A C26A H26A 109.5 . .
N21A C26A H26B 109.5 . .
C25A C26A H26B 109.5 . .
H26A C26A H26B 108.1 . .
C4B O1B Mg1 126.1(2) . .
C1B O11B Mg1 131.9(2) . .
C8B O2B C11B 113.5(2) . .
C2B N1B C9B 119.9(3) . .
C2B N1B C12B 123.0(3) . .
C9B N1B C12B 116.6(2) . .
C7B N21B C22B 120.2(3) . .
C7B N21B C26B 116.8(2) . .
C22B N21B C26B 112.4(2) . .
C23B N24B C14B 110.0(2) . .
C23B N24B C25B 109.3(2) . .
C14B N24B C25B 110.4(3) . .
O12B C1B O11B 123.2(3) . .
O12B C1B C3B 117.9(3) . .
O11B C1B C3B 118.9(3) . .
N1B C2B C3B 124.2(3) . .
N1B C2B H2B 117.9 . .
C3B C2B H2B 117.9 . .
C2B C3B C4B 119.1(3) . .
C2B C3B C1B 116.3(3) . .
C4B C3B C1B 124.6(3) . .
O1B C4B C3B 125.1(3) . .
O1B C4B C10B 118.4(3) . .
C3B C4B C10B 116.5(3) . .
C6B C5B C10B 118.2(3) . .
C6B C5B H5B 120.9 . .
C10B C5B H5B 120.9 . .
F1B C6B C5B 117.9(3) . .
F1B C6B C7B 117.2(3) . .
C5B C6B C7B 124.8(3) . .
C8B C7B N21B 125.4(3) . .
C8B C7B C6B 116.0(3) . .
N21B C7B C6B 118.5(3) . .
O2B C8B C7B 117.8(3) . .
O2B C8B C9B 122.0(3) . .
C7B C8B C9B 120.1(3) . .
N1B C9B C10B 119.6(3) . .
N1B C9B C8B 119.6(3) . .
C10B C9B C8B 120.8(3) . .
C9B C10B C5B 119.2(3) . .
C9B C10B C4B 120.6(3) . .
C5B C10B C4B 120.2(3) . .
O2B C11B C12B 109.4(2) . .
O2B C11B H11C 109.8 . .
C12B C11B H11C 109.8 . .
O2B C11B H11D 109.8 . .
C12B C11B H11D 109.8 . .
H11C C11B H11D 108.2 . .
N1B C12B C11B 105.7(2) . .
N1B C12B C13B 113.4(2) . .
C11B C12B C13B 113.2(3) . .
N1B C12B H12B 108.1 . .
C11B C12B H12B 108.1 . .
C13B C12B H12B 108.1 . .
C12B C13B H13D 109.5 . .
C12B C13B H13E 109.5 . .
H13D C13B H13E 109.5 . .
C12B C13B H13F 109.5 . .
H13D C13B H13F 109.5 . .
H13E C13B H13F 109.5 . .
N24B C14B H14D 109.5 . .
N24B C14B H14E 109.5 . .
H14D C14B H14E 109.5 . .
N24B C14B H14F 109.5 . .
H14D C14B H14F 109.5 . .
H14E C14B H14F 109.5 . .
N21B C22B C23B 108.4(3) . .
N21B C22B H22C 110.0 . .
C23B C22B H22C 110.0 . .
N21B C22B H22D 110.0 . .
C23B C22B H22D 110.0 . .
H22C C22B H22D 108.4 . .
```

```
N24B C23B C22B 111.4(3) . .
N24B C23B H23C 109.4 . .
C22B C23B H23C 109.4 . .
N24B C23B H23D 109.4 . .
C22B C23B H23D 109.4 . .
H23C C23B H23D 108.0 . .
N24B C25B C26B 110.6(3) . .
N24B C25B H25C 109.5 . .
C26B C25B H25C 109.5 . .
N24B C25B H25D 109.5 . .
C26B C25B H25D 109.5 . .
H25C C25B H25D 108.1 . .
N21B C26B C25B 109.5(2) . .
N21B C26B H26C 109.8 . .
C25B C26B H26C 109.8 . .
N21B C26B H26D 109.8 . .
C25B C26B H26D 109.8 . .
H26C C26B H26D 108.2 . .
H3W O2W H4W 110(4) . .
H1W O1W H2W 101(3) . .

loop_
 _geom_torsion_atom_site_label_1
 _geom_torsion_atom_site_label_2
 _geom_torsion_atom_site_label_3
 _geom_torsion_atom_site_label_4
 _geom_torsion
 _geom_torsion_site_symmetry_1
 _geom_torsion_site_symmetry_2
 _geom_torsion_site_symmetry_3
 _geom_torsion_site_symmetry_4
 _geom_torsion_publ_flag
O11A Mg1 O1A C4A -30.0(2) . . . .
O1B Mg1 O1A C4A 29(3) . . . .
O11B Mg1 O1A C4A 148.4(2) . . . .
O2M Mg1 O1A C4A -121.4(2) . . . .
O1M Mg1 O1A C4A 58.9(2) . . . .
O1B Mg1 O11A C1A -155.0(3) . . . .
O1A Mg1 O11A C1A 23.3(3) . . . .
O11B Mg1 O11A C1A -106(3) . . . .
O2M Mg1 O11A C1A 114.2(3) . . . .
O1M Mg1 O11A C1A -64.8(3) . . . .
Mg1 O11A C1A O12A 170.4(2) . . . .
Mg1 O11A C1A C3A -7.7(4) . . . .
C9A N1A C2A C3A 0.3(4) . . . .
C12A N1A C2A C3A -179.2(3) . . . .
N1A C2A C3A C4A -2.1(4) . . . .
N1A C2A C3A C1A 177.0(3) . . . .
O12A C1A C3A C2A -9.3(4) . . . .
O11A C1A C3A C2A 168.9(3) . . . .
O12A C1A C3A C4A 169.8(3) . . . .
O11A C1A C3A C4A -12.0(4) . . . .
Mg1 O1A C4A C3A 23.2(4) . . . .
Mg1 O1A C4A C10A -156.77(19) . . . .
C2A C3A C4A O1A -177.6(3) . . . .
C1A C3A C4A O1A 3.3(5) . . . .
C2A C3A C4A C10A 2.4(4) . . . .
C1A C3A C4A C10A -176.7(3) . . . .
C10A C5A C6A F1A -176.3(2) . . . .
C10A C5A C6A C7A 2.4(5) . . . .
C26A N21A C7A C8A -68.8(4) . . . .
C22A N21A C7A C8A 151.4(3) . . . .
C26A N21A C7A C6A 113.6(4) . . . .
C22A N21A C7A C6A -26.1(4) . . . .
C5A C6A C7A C8A -5.9(4) . . . .
F1A C6A C7A C8A 172.8(3) . . . .
C5A C6A C7A N21A 171.7(3) . . . .
F1A C6A C7A N21A -9.6(4) . . . .
C11A O2A C8A C7A 150.2(3) . . . .
C11A O2A C8A C9A -33.6(4) . . . .
N21A C7A C8A O2A 2.7(4) . . . .
C6A C7A C8A O2A -179.5(3) . . . .
N21A C7A C8A C9A -173.4(2) . . . .
C6A C7A C8A C9A 4.4(4) . . . .
C2A N1A C9A C10A 1.1(4) . . . .
C12A N1A C9A C10A -179.4(3) . . . .
C2A N1A C9A C8A -175.5(3) . . . .
C12A N1A C9A C8A 4.0(4) . . . .
O2A C8A C9A C10A -175.7(3) . . . .
C7A C8A C9A C10A 0.3(4) . . . .
O2A C8A C9A N1A 0.9(4) . . . .
C7A C8A C9A N1A 176.9(3) . . . .
N1A C9A C10A C5A 179.3(3) . . . .
C8A C9A C10A C5A -4.1(4) . . . .
N1A C9A C10A C4A -0.7(4) . . . .
C8A C9A C10A C4A 176.0(3) . . . .
C6A C5A C10A C9A 2.8(4) . . . .
C6A C5A C10A C4A -177.3(3) . . . .
O1A C4A C10A C9A 178.9(3) . . . .
C3A C4A C10A C9A -1.1(4) . . . .
O1A C4A C10A C5A -1.1(4) . . . .
C3A C4A C10A C5A 179.0(2) . . . .
C8A O2A C11A C12A 61.4(3) . . . .
C2A N1A C12A C13A 76.6(3) . . . .
C9A N1A C12A C13A -103.0(3) . . . .
C2A N1A C12A C11A -158.2(2) . . . .
C9A N1A C12A C11A 22.3(3) . . . .
O2A C11A C12A N1A -54.0(3) . . . .
O2A C11A C12A C13A 69.6(3) . . . .
C7A N21A C22A C23A -162.5(3) . . . .
C26A N21A C22A C23A 55.7(4) . . . .
C25A N24A C23A C22A 61.2(4) . . . .
C14A N24A C23A C22A -176.7(3) . . . .
N21A C22A C23A N24A -58.9(4) . . . .
C23A N24A C25A C26A -59.4(3) . . . .
C14A N24A C25A C26A 179.0(2) . . . .
C7A N21A C26A C25A 162.8(3) . . . .
C22A N21A C26A C25A -54.9(4) . . . .
N24A C25A C26A N21A 56.4(3) . . . .
O11A Mg1 O1B C4B -155.7(2) . . . .
O1A Mg1 O1B C4B 145(3) . . . .
O11B Mg1 O1B C4B 25.8(2) . . . .
O2M Mg1 O1B C4B -64.3(2) . . . .
O1M Mg1 O1B C4B 115.4(2) . . . .
O11A Mg1 O11B C1B -62(3) . . . .
O1B Mg1 O11B C1B -12.9(3) . . . .
O1A Mg1 O11B C1B 168.9(2) . . . .
O2M Mg1 O11B C1B 77.9(3) . . . .
O1M Mg1 O11B C1B -103.2(3) . . . .
Mg1 O11B C1B O12B 177.7(2) . . . .
Mg1 O11B C1B C3B -2.0(4) . . . .
C9B N1B C2B C3B 0.4(4) . . . .
C12B N1B C2B C3B 172.9(3) . . . .
N1B C2B C3B C4B -1.1(4) . . . .
N1B C2B C3B C1B -179.7(2) . . . .
O12B C1B C3B C2B 11.9(4) . . . .
O11B C1B C3B C2B -168.3(3) . . . .
O12B C1B C3B C4B -166.7(3) . . . .
```

```
O11B C1B C3B C4B 13.1(4) . . . .
Mg1 O1B C4B C3B -24.4(4) . . . .
Mg1 O1B C4B C10B 158.36(19) . . . .
C2B C3B C4B O1B -177.7(3) . . . .
C1B C3B C4B O1B 0.8(4) . . . .
C2B C3B C4B C10B -0.4(4) . . . .
C1B C3B C4B C10B 178.1(2) . . . .
C10B C5B C6B F1B -173.7(2) . . . .
C10B C5B C6B C7B 5.0(4) . . . .
C22B N21B C7B C8B -31.4(4) . . . .
C26B N21B C7B C8B 110.6(3) . . . .
C22B N21B C7B C6B 145.3(3) . . . .
C26B N21B C7B C6B -72.6(4) . . . .
F1B C6B C7B C8B 179.6(2) . . . .
C5B C6B C7B C8B 1.0(4) . . . .
F1B C6B C7B N21B 2.5(4) . . . .
C5B C6B C7B N21B -176.1(3) . . . .
C11B O2B C8B C7B -166.8(3) . . . .
C11B O2B C8B C9B 15.4(4) . . . .
N21B C7B C8B O2B -9.0(4) . . . .
C6B C7B C8B O2B 174.2(3) . . . .
N21B C7B C8B C9B 168.8(3) . . . .
C6B C7B C8B C9B -8.0(4) . . . .
C2B N1B C9B C10B 1.8(4) . . . .
C12B N1B C9B C10B -171.1(3) . . . .
C2B N1B C9B C8B -179.2(3) . . . .
C12B N1B C9B C8B 7.8(4) . . . .
O2B C8B C9B N1B 8.2(4) . . . .
C7B C8B C9B N1B -169.5(3) . . . .
O2B C8B C9B C10B -172.9(3) . . . .
C7B C8B C9B C10B 9.4(4) . . . .
N1B C9B C10B C5B 175.6(3) . . . .
C8B C9B C10B C5B -3.3(4) . . . .
N1B C9B C10B C4B -3.3(4) . . . .
C8B C9B C10B C4B 177.7(3) . . . .
C6B C5B C10B C9B -3.7(4) . . . .
C6B C5B C10B C4B 175.3(3) . . . .
O1B C4B C10B C9B -179.9(3) . . . .
C3B C4B C10B C9B 2.6(4) . . . .
O1B C4B C10B C5B 1.1(4) . . . .
C3B C4B C10B C5B -176.4(3) . . . .
C8B O2B C11B C12B -52.7(3) . . . .
C2B N1B C12B C11B 144.7(3) . . . .
C9B N1B C12B C11B -42.6(3) . . . .
C2B N1B C12B C13B 20.1(4) . . . .
C9B N1B C12B C13B -167.1(2) . . . .
O2B C11B C12B N1B 65.1(3) . . . .
O2B C11B C12B C13B -170.3(2) . . . .
C7B N21B C22B C23B -159.5(3) . . . .
C26B N21B C22B C23B 56.9(3) . . . .
C14B N24B C23B C22B -178.8(3) . . . .
C25B N24B C23B C22B 59.8(3) . . . .
N21B C22B C23B N24B -58.2(4) . . . .
C23B N24B C25B C26B -58.8(3) . . . .
C14B N24B C25B C26B -180.0(3) . . . .
C7B N21B C26B C25B 158.0(3) . . . .
C22B N21B C26B C25B -57.1(3) . . . .
N24B C25B C26B N21B 57.1(3) . . . .

loop_
 _geom_hbond_atom_site_label_D
 _geom_hbond_atom_site_label_H
 _geom_hbond_atom_site_label_A
 _geom_hbond_distance_DH
 _geom_hbond_distance_HA
 _geom_hbond_distance_DA
 _geom_hbond_angle_DHA
 _geom_hbond_site_symmetry_A
O1M H12M O12B  0.93(4) 1.79(4)
2.716(3) 172(3) 2_646
O1M H11M O1W  0.83(5) 1.96(5)
2.749(4) 158(4) 2_646
O2M H21M O12A  0.81(3) 1.95(3)
2.755(3) 175(4) 2_556
O2M H22M O2W  0.97(5) 1.76(5)
2.676(4) 156(3) 1_565
O2W H3W O11A  0.80(4) 2.07(4)
2.869(3) 171(4) 2_546
O2W H4W O12A  0.97(6) 1.81(6)
2.725(3) 156(5) .
O1W H1W O12B  1.00(3) 1.79(3)
2.775(3) 169(3) 2_646
O1W H2W O11B  0.90(4) 1.95(4)
2.843(3) 178(4) .
```